SENRA Academic Publishers, Burnaby, British Columbia
Vol. 3, No. 1, pp. 675-690, 2009
ISSN: 1715-9997

Canadian Journal of pure&applied sciences

ACOUSTIC WAVES WITH THE IN-PLANE POLARIZATION IN PIEZOELECTRIC CUBIC STRUCTURES

AA Zakharenko
International Institute of Zakharenko Waves
660037, Krasnoyarsk-37, 17701, Krasnoyarsk, Russia

ABSTRACT

In this paper, calculations of the phase velocity V_{ph} of the dispersive nine-partial Rayleigh type waves (RTW9) were introduced in dependence on the kh (k is the wavenumber, and h is the layer thickness). The layered systems, consisting of a layer of $Bi_{12}SiO_{20}$ on a substrate of $Bi_{12}GeO_{20}$, and the reverse configurations were investigated. The calculated dispersion curves of the RTW9 lowest-order modes with both metallized and free surfaces have shown the existence of the non-dispersive nine-partial Zakharenko type waves (ZTW9) polarized like the Rayleigh waves. The non-dispersive ZTW9-waves split the RTW9 lowest-order modes into sub-modes with different dispersions, $V_{ph} > V_g$ and $V_{ph} < V_g$, where V_g is the group velocity. The RTW9 phase velocity V_{ph} is confined within a narrow V_{ph}-range that can be convenient for some technical devices. Also, cubic crystals with strong piezoelectric effect can be used for different cubic-structure magnetoelectric devices. It was found that the coefficient of electromechanical coupling (CEMC) K^2 for the RTW9 first type has its maximum value at $kh \sim 5$ for the structure $Bi_{12}SiO_{20}/Bi_{12}GeO_{20}$. The second type of RTW9-waves was also studied, which can propagate only in the structure $Bi_{12}SiO_{20}/Bi_{12}GeO_{20}$, because there is the condition $V_t(Bi_{12}GeO_{20}) > V_t(Bi_{12}SiO_{20})$ for the speed V_t of the bulk transverse wave, $V_t = [(C_{55}/\rho)(1 + K_0^2)]^{1/2}$ with $K_0^2 = e_{15}^2 / C_{55}\varepsilon_{11}$. It was also discussed the existence possibility of new supersonic surface waves with the in-plane polarization and $V_{ph} \sim V_l$, where V_l represents the speed of the bulk longitudinal wave. Also, a calculation method with short computer program is described introducing the transverse and longitudinal dynamic CEMCs K_{Dt} and K_{Dl}. For comparison with [110] direction, the 20^0-x_2-rotated direction was also studied concerning propagation of the first and second types of pure RTW9-waves. Here, the existence of RTW9 second type depends on the velocity equivalents of the layer and substrate, but not on the corresponding velocities V_t, and solutions for the $V_{ph} > V_t$ were also found.

PACS: 51.40.+p, 62.65.+k, 68.35.Gy, 68.35.Iv, 68.60.Bs, 74.25.Ld

Keywords: layered systems, piezoelectric cubic crystals, dispersive Rayleigh waves, non-dispersive Zakharenko waves.

INTRODUCTION

Studying the propagation of elastic waves, especially the surface acoustic wave (SAW), in layered piezoelectric media have been of great interest since films deposited on supporting substrates are generally a requisite for acoustic devices (Nayfeh, 1991). Typically, a layered structure consists of two layers of different materials. Some technical devices, for instance, dispersive delay lines (Lardat *et al*., 1971) using layered structures to support propagation of dispersive waves require choosing materials for both the layer and substrate, in order to have a large range for the phase velocity V_{ph} in which dispersive waves can be confined. However, for some technical devices, a very narrow V_{ph}-range for dispersive waves can be preferable (Shiosaki *et al*., 1980) demonstrating a weak dependence of the dispersive wave V_{ph} on the non-dimensional value of kh, where k is the wavenumber in direction of wave propagation and h is the layer thickness. Also, (multi)-layered systems can be used for parameter optimization of technical devices, for example, see (Dvoesherstov *et al*., 2003). There is the famous and classical book (Dieulesaint and Royer, 1980) on elastic waves in solids and their applications to signal processing. Also, an additional literature on crucial applications of SAWs can be found in (Henaff *et al*., 1982).

This paper relates to the studying the so-called "pure" dispersive nine-partial Rayleigh type waves (RTW9) in the layered systems, consisting of strongly piezoelectric cubic crystals $Bi_{12}SiO_{20}$ and $Bi_{12}GeO_{20}$, accounting the piezoelectric effect. Particularly, the attention of this work is paid to other possibilities to find dispersive SAWs with the Rayleigh-wave polarization in addition to the well-known surface Rayleigh waves (Rayleigh, 1885). It is thought that the two-layer systems using the crystals $Bi_{12}SiO_{20}$ and $Bi_{12}GeO_{20}$ can be readily manufactured. It is noted that over several hundred piezoelectric ceramics (composites) are known, for example, see (Pohanka and Smith, 1988). Today, they are widely used for different applications such as filters and sensors, as well as actuators and ultrasonic generators. Concerning fabrication of a structure consisting of two dissimilar crystals, a process called wafer bonding (Goesele and

*Corresponding author email: aazaaz@inbox.ru

Tong, 1998; Alexe and Goesele, 2003) is commonly used in the semiconductor industry allowing two different materials to be rigidly and permanently bonded along a plane interface.

In this paper, the RTW9-waves propagate in [110] direction for both materials as shown in figure 1. The so-called work coordinate system $\{x_1, x_2, x_3\}$ in the Figure was obtained by 45^0-rotation around the Z-axis of the so-called crystallographic coordinate system with the $\{X, Y, Z\}$ axes corresponding to [100], [010], and [001] directions, respectively. It is noted that both the x_1 and x_3-axes lie in the sagittal plane in Figure 1, and the x_3-axis is perpendicular to the Figure plane, where the vector **N** is parallel to the surface normal, and the vector **M** is directed towards the propagation direction. The existence possibility of "pure" RTW6 and RTW9-waves was studied in the very famous works (Farnell and Adler, 1972; Lardat *et al*., 1971). In the studied layered systems, a weak dependence $V_{ph}(kh)$ can occur with peculiarities such as the phenomenon called the non-dispersive Zakharenko type wave (ZTW) recently discovered in (Zakharenko, 2005[a]). The non-dispersive ZTW-wave can exist in complex systems, which possess dependence of the V_{ph} on both the wavenumber k and the angular frequency ω. For example, the non-dispersive ZTW-waves can split some higher-order modes of Lamb type waves in anisotropic plates (Anisimkin, 2004; Solie and Auld, 1973; Parygin *et al*., 2000) into several sub-modes (modes). It is noted that Anisimkin in 2004 has thought that higher-order modes of Lamb type waves possessing the non-dispersive ZTW-waves represent modes of new dispersive waves, because Lamb (type) waves are defined as dispersive waves. It is well-known that there are many types of dispersive waves polarized in the sagittal plane such as dispersive Rayleigh and Lamb type waves, as well as dispersive leaky Sezawa waves. The non-dispersive Stoneley type waves propagating at the interface of two solids can also have the "in-plane" polarization. Love type waves (Love, 1911) and surface Bleustein-Gulyaev (BG) type waves (Bleustein, 1968; Gulyaev, 1969) possess unique polarization perpendicular to the sagittal plane. However, the non-dispersive ZTW-waves representing extreme points of $V_{ph}(kh)$ can also split a mode of dispersive BG-waves (Liu *et al*., 2003). It is noted that the non-dispersive ZTW-waves were understood as corresponding dispersive waves in all papers before the work (Zakharenko, 2005[a]).

Note that a dispersive mode can possess three non-dispersive ZTW-waves that were schematically shown by Ivanov and Kessenikh (1987) for non-piezoelectric materials. Probably, their result shows how many non-dispersive ZTW-waves can exist in the same mode of dispersive wave, omitting the fact that a lowest-order mode can split. Therefore, they introduced their results as being one dispersive mode, and their theory must be verified in experiments. It is thought that only structures with a relatively weak dependence $V_{ph}(kh)$ can possess non-dispersive ZTW-waves. It is thought that a layered system with the non-dispersive ZTW-waves could be used in technical devices instead of a monocrystal (several monocrystals). In addition, Zhang and Lu (2003) have also found that the lowest-order mode can split into several sub-modes that could be called the Zhang-Lu law. However, their result does not give information about where this splitting occurs and how many sub-modes can exist.

Several layered systems are today well-known possessing a weak dependence $V_{ph}(kh)$ in the lowest-order mode of dispersive RTW-waves. Cubic crystals are crystals with zero temperature coefficients, and they can have strong piezoelectric coupling. However, transversely-isotropic crystals are widely studied in contrast to the cubic crystals studied in this paper. For example, there is a strong interest in the layered system, consisting of a weakly-piezoelectric AlN-layer on a fused-quartz–substrate, for SAW-devices with a weak dependence $V_{ph}(kh)$, see (Volyansky *et al*., 1987; Bondarenko *et al*., 1983; Shiosaki *et al*., 1980; Tsubouchi and Mikoshiba, 1985). In the work of Volyansky *et al*. (1987) a calculation method was simplified omitting the piezoelectric effect, and a close correlation between theoretical calculations and experimental measurements of the V_{ph} was obtained. A very interesting case was treated in the work of Solie (1971) for the layered system, consisting of a fused-quartz–layer on a (YZ)-$LiNbO_3$–substrate. In the case by Solie (1971), the first sub-mode is also confined in a narrow V_{ph}-range ~ 3 ms^{-1} at small values of kh, and the next sub-modes are confined in larger V_{ph}-ranges interrupting within the kh-range: $1.2 < kh < 3.35$. The layered system, consisting of a ZnO-layer on a weakly-piezoelectric GaAs-substrate, is also interesting because it is possible to monolithically integrate such SAW-devices with GaAs-electronics. The lowest-order mode with no shorting plane for that layered system was recently calculated in (Zhang *et al*., 2001). Here, the V_{ph}-range is more than 300 ms^{-1} for the second sub-mode and smaller than 2.5 ms^{-1} for the first sub-mode with $V_g > V_{ph}$ at small values of kh. Schmidt and Voltmer (1969) have shown the lowest-order mode for the two-layer structure, consisting of a piezoelectric CdS-layer on a fused-quartz–substrate, where there is a relatively large dependence $V_{ph}(kh)$. The same $V_{ph}(kh)$ was found in (Nakamura and Hanaoka, 1993) by studying the layered system, consisting of a ZnO-layer on a 128^0-rotated Y-cut $LiNbO_3$-substrate. In both latter cases, the peculiarities were not found in the RTW9 lowest-order mode. In the layered system, consisting of the isotropic silicon–layer on the ZnO-substrate treated in (Farnell, 1978) the V_{ph} of dispersive RTW-wave is confined between the RTW-wave for the ZnO-substrate and the corresponding bulk transverse waves for the substrate, because the latter is the V_{ph} upper

limit. The next section describes theory of propagation of dispersive waves with the in-plane polarization. The third section describes different boundary conditions. Results and discussions are written in the fourth section. The fifth section discusses the other possibilities of finding waves with the in-plane polarization in addition to the dispersive Rayleigh type waves. For comparison with [110] direction, the sixth section describes theoretical results of studying in-plane polarized waves in more complicated case of monoclinic symmetry material constants when the theory of section 2 cannot be used.

THEORY

In different layered structures, consisting of piezoelectric materials, propagation equations are written, according to (Farnell and Adler, 1972; Lardat *et al*., 1971), with components of both the mechanic displacements U_i and the electric field E_J. The constitutive equations for a piezoelectric material can be expressed in terms of the strains and the electric field. Strains are related to mechanic displacements: $\tau_{ij} = (U_{i,j} + U_{j,i})/2$ (Lyamov, 1983). The governing mechanical equilibrium is $ST_{ij,j} = 0$, and the governing electrostatic equilibrium is $D_{i,i} = 0$, where ST_{ij} and D_i are the stress tensor and electric displacement components, respectively. The comma denotes coordinate differentiation with respect to x_i. Each medium possesses the elastic C_{pqrw} and piezoelectric e_{pqr} coefficients, the dielectric constants ε_{pq}, and the medium density ρ. Because dispersive Rayleigh-polarized waves are treated in this paper, only two components of the mechanical displacements, U_1 along the x_1-axis and U_3 along the x_3-axis in Figure 1, are used which lie in the sagittal plane. The components U_1 and U_3 as well as the components E_1 and E_3 can be written in view of plane waves:

$$U_{1,3} = U^0_{1,3} \exp[\mathrm{j}(k_1 x_1 + k_3 x_3 - \omega t)]$$
$$E_{1,3} = E^0_{1,3} \exp[\mathrm{j}(k_1 x_1 + k_3 x_3 - \omega t)] \qquad (1)$$

where k_1 and k_3 are components of the wavevector $\mathbf{K}_s$ along the x_1-axis and the x_3-axis, respectively, and ω and t are the cycle frequency and time; $\mathrm{j} = (-1)^{1/2}$. $U^0_{1,3}$ and $E^0_{1,3}$ are initial amplitudes. The electric field E_J is defined by the electric potential ϕ: $E_J = -\partial\phi/\partial x_J$, $J = 1, 2, 3$.

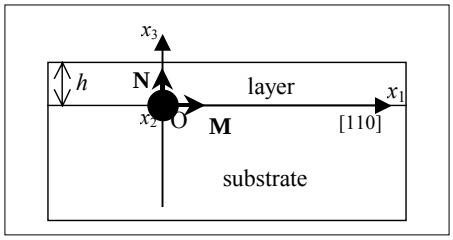

Fig. 1. The propagation direction in the layered system, where the vectors **N** and **M** are directed along the surface normal and propagation direction, respectively. Here the so-called work coordinate system $\{x_1, x_2, x_3\}$ is used, where the x_2-axis is perpendicular to the Figure plane and the sagittal plane (x_1Ox_3).

The piezoelectromechanical waves with polarization in the sagittal plane can propagate in a piezoelectric medium when the sagittal plane coincides with the symmetry plane of the medium, according to (Farnell and Adler, 1972; Lardat *et al*., 1971). In such propagation directions, for example, [110] propagation direction for cubic crystals, there are the following zero GL_{rw}-components in the Green-Christoffel (GL) equation, $(GL_{rw} - \delta_{rw}\rho V_{ph})U_r = 0$ (Farnell and Adler, 1972; Farnell, 1978; Lyamov, 1983): $GL_{21} = GL_{12} = GL_{32} = GL_{23} = GL_{24} = GL_{42} = 0$. In the GL-equation, r and w run from 1 to 4, δ_{rw} is the Kronecker delta for $r < 4$ and $w < 4$, $\delta_{rw} = 0$ for $r \neq w$ and $\delta_{44} = 0$, $U_r = \{U_1, U_2, U_3, \phi\}$. V_{ph} is the phase velocity, $V_{ph} = \omega/k$, where k is the wavenumber in direction of wave propagation. Therefore, the following equations can be written for the in-plane polarized waves:

$$\begin{pmatrix} C_{55}n_3^2 + C_{11}A_l^2 & (C_{13}+C_{55})n_3 & (e_{15}+e_{31})n_3 \\ (C_{13}+C_{55})n_3 & C_{33}n_3^2 + C_{55}A_t^2 & e_{15} \\ (e_{15}+e_{31})n_3 & e_{15} & -\varepsilon_{11} - \varepsilon_{33}n_3^2 \end{pmatrix} \begin{pmatrix} U_1 \\ U_3 \\ \phi \end{pmatrix} = 0 \qquad (2)$$

In equation (2), $C_{11} \neq C_{33}$, C_{55}, and C_{13} are the corresponding non-zero components of the elasticity tensor (Voigt notation). $e_{15} = e_{31}$ and $\varepsilon_{11} = \varepsilon_{33}$ are the non-zero piezoelectric and dielectric constants, respectively. It is noted that for cubic crystals in [110] propagation direction there is the following relationship between the elastic constants C_{11} and C_{33}: $C_{11} = C_{55} + (C_{33} + C_{13})/2$ (Stoneley, 1955; Tursunov, 1967). Also, in Eq. (2) there are $A_l^2 = 1 - (V_{ph}/V_l)^2$ and $A_t^2 = 1 - (V_{ph}/V_{t5})^2$. $V_l = [C_{11}/\rho]^{1/2}$ and $V_{t5} = [C_{55}/\rho]^{1/2}$ are the so-called velocity equivalents for [110] direction. However, they are the speeds of the bulk longitudinal and transverse waves for [100] direction, respectively. For [110] direction, the speed V_t of the bulk transverse wave is equal to $V_t = [(C_{55}/\rho)(1 + K_0^2)]^{1/2}$, and the bulk longitudinal wave propagates with the speed $V_{l3} = [C_{33}/\rho]^{1/2}$. K_0^2 is called the static coefficient of electromechanical coupling (CEMC): $K_0^2 = e_{15}^2 / C_{55}\varepsilon_{11}$. However, in the case of $C_{11} = C_{33}$, for example, in [100] propagation direction of cubic crystals (Zakharenko, 2005[a]) there is $V_{l3} = V_l$. Also, many non-cubic acoustic crystals with $C_{11} \sim C_{33}$ can be readily found in (Landolt-Boernstein Int. Tables, 1985; Blistanov *et al*., 1982).

For definition, the non-dimensional complex component n_3 is $n_3 = k_3/k$, and there are $n_1 = 1$ and $n_2 = 0$ in Eq. (2). For piezoelectric cubic crystals, the material constants in [100] direction $\{(C_{11} = C_{22} = C_{33}, C_{12} = C_{13} = C_{23}, C_{44} = C_{55} = C_{66}); (e_{14} = e_{25} = e_{36}); (\varepsilon_{11} = \varepsilon_{22} = \varepsilon_{33}); \rho; (V_L, V_{FT} = V_{ST}, V_{RTW6})\}$ transform into the following material constants in [110] direction $\{(C_{11} = C_{22}, C_{33}, C_{12}, C_{13} = C_{23}, C_{44} = C_{55}, C_{66}); (e_{15} = e_{31} = -e_{32} = -e_{24}); (\varepsilon_{11} = \varepsilon_{22} = \varepsilon_{33}); \rho; (V_L, V_{FT}, V_{ST}, V_{RTW9})\}$, where V_L, V_{FT} , and V_{ST} represent the speeds of the bulk longitudinal, fast, and slow transverse waves, respectively: $V_{FT} = (C_{66}/\rho)^{1/2}$ and $V_{ST} = [(C_{55}/\rho)(1 + K_0^2)]^{1/2}$. The material constants for the

cubic crystals $Bi_{12}SiO_{20}$ and $Bi_{12}GeO_{20}$ are given in table 1 for both propagation directions.

For convenience, the corresponding determinant for the determination of the complex component n_3 can be transformed from Eq. (2) into the following view, after some transformations:

$$\begin{vmatrix} C_{55}m + C_{11}A_l^2 & (C_{13}+C_{55})m & 2m \\ (C_{13}+C_{55}) & C_{33}m + C_{55}A_t^2 & 1 \\ 2 & 1 & -a(1+m) \end{vmatrix} = 0 \qquad (3)$$

with $m = n_3^2$ and $a = 1/(K_0^2 C_{55})$.

Expanding the determinant (3), the secular equation is obtained representing a sixth order polynomial for determination of the eigenvalues $n_3^{(N)}$, where the index N runs from 1 to 6. After some transformations, the obtained polynomial from (3) can be shown as follows:

$$m^3 + Am^2 + Bm + C = 0 \qquad (4)$$

where

$$A = \left[\frac{C_{11}}{C_{33}}A_l^2 + A_t^2 + C^2\right] + 1 + 4K_0^2$$

$$B = \left[\frac{C_{11}}{C_{33}}A_l^2 + A_t^2 + C^2\right] + \frac{C_{11}}{C_{33}}A_l^2 A_t^2 + K_{Dt} \qquad (5)$$

$$C = \frac{C_{11}}{C_{33}}A_l^2 A_t^2 + K_{Dl}$$

The coefficients A, B, and C in (5) consist of both the corresponding elastic anisotropy terms and the corresponding terms K_0^2, K_{Dt}, and K_{Dl} coupled with the piezoelectricity influence. The elastic constants are combined in the anisotropy term C^2 (Zakharenko, 2005[a]; Zakharenko, 2006) which appears in the square brackets of the coefficients A and B in (5) and has the following view for the studied direction:

Table 1. The characteristics for $Bi_{12}SiO_{20}$ and $Bi_{12}GeO_{20}$. The piezoelectric e_{14} and dielectric ε_{11} material constants are the same in both propagation directions. The corresponding elastic constants C_{ij} are given in [N/m^2] $\times 10^{10}$ and all the velocities are in [m/s].

[100] propagation direction									
Material	ρ, [kg/m^3]	C_{11}	C_{12}	C_{44}	e_{14}, [C/m^2]	ε_{11}, 10^{-10} [F/m]	V_t	V_l	V_{RTW2}
$Bi_{12}SiO_{20}$	9070	12.962	2.985	2.451	1.122	3.63735	1643.87	3780.35	1606.08
$Bi_{12}GeO_{20}$	9200	12.852	2.934	2.562	0.983	3.336	1668.77	3737.59	1626.11
[110] propagation direction									
Material	C_{11}	C_{33}	C_{13}	C_{55}	C_{66}	V_l	V_{ST}	V_{FT}	V_{RTW3}
$Bi_{12}SiO_{20}$	10.4245	12.962	2.985	2.451	4.9885	3390.19	1756.10	2345.21	1681.50
$Bi_{12}GeO_{20}$	10.455	12.852	2.934	2.562	4.959	3371.07	1760.58	2321.68	1683.78

Table 2. The non-dimensional anisotropy term C^2 and the velocities V_t, V_l, and V^{th} for the piezoelectric cubic crystals in [100] propagation direction of (001) cut, in which Rayleigh-polarized waves do not coupled with the electric potential.

№	Cubic crystal	Structure type	Density ρ [kg/m^3]	Elastic constants $C_{ij,}$ 10^{10} [N/m^2]			Anisotropy factor η	Anisotropy term C^2	Velocity V_t [m/s]	Velocity V_l [m/s]	Velocity V^{th} [m/s]
				C_{11}	C_{44}	C_{12}					
Piezoelectric class 23											
1.	$NaClO_3$	$NaClO_3$	2490	4.887	1.173	1.675	0.73	0.99	2170	4430	3370
2.	$NaBrO_3$	$NaClO_3$	3330	5.708	1.525	1.695	0.76	0.82	2140	4140	3192
Piezoelectric class $\bar{4}3m$											
3.	GaP	ZnS	4301	14.110	6.260	7.030	1.77	– 1.30	3815	5728	2657
4.	GaAs	ZnS	5316	11.810	5.940	5.320	1.83	– 1.32	3343	4713	2249
5.	β-ZnS	ZnS	4091	10.460	4.610	4.640	1.58	– 1.07	3310	4897	2645
6.	ZnSe	ZnS	5264	8.720	3.920	5.240	2.25	– 1.78	2729	4070	1063
7.	InSb	ZnS	5790	6.720	3.040	3.670	1.99	– 1.54	2291	3407	1289
8.	CuCl	ZnS	3530	4.500	1.342	3.711	3.40	– 2.58	1950	3570	i1303
9.	CuBr	ZnS	4720	4.624	1.413	3.512	2.54	– 2.13	1730	3130	i546
10.	ZnTe	ZnS	5636	7.130	3.120	4.070	2.04	– 1.60	2353	3557	1241
11.	CdTe	ZnS	5849	5.351	1.994	3.681	2.39	– 1.93	1846	3025	417
12.	Tl_3TaS_4	-	6790	4.910	0.320	1.130	0.17	12.07	687	2689	2497
13.	Tl_3TaSe_4	-	7280	4.190	0.410	1.400	0.29	6.41	751	2399	2078
14.	$Bi_4(GeO_4)_3$	eulytine	7120	11.580	4.360	2.700	0.98	0.03	2475	4033	3006
15.	$Bi_4(SiO_4)_3$	eulytine	6800	13.570	5.180	2.270	0.92	0.21	2760	4467	3491

$$C^2 = \left[(C_{11} - C_{55})(C_{33} - C_{55}) - (C_{13} + C_{55})^2\right] / C_{33}C_{55} \quad (6)$$

It is noted that the C^2 in Eq. (6) is a universal non-dimensional crystal characteristics, which can be suitable for all crystal symmetries, except the triclinic and monoclinic symmetries. However, for a particular case of C_{15}, $C_{35} << C_{55}$, C_{13}, C_{11}, and C_{33}, the C^2 is also suitable for the symmetries.

The corresponding piezoelectric parts in (5) coupled with the static CEMC K_0^2 are as follows: $(4K_0^2)$ or $(1 + 4K_0^2)$ in the coefficient A, the so-called dynamic CEMCs K_{Dt} and K_{Dl} in the coefficients B and C, respectively. The introduced non-dimensional characteristics K_{Dt} and K_{Dl} depend on both the cubic crystal anisotropy and the V_{ph}:

$$K_{Dt} = \frac{K_0^2}{C_{33}}\left[4C_{55}A_t^2 - 4C_{13} - 3C_{55}\right] \quad K_{Dl} = K_0^2\frac{C_{11}}{C_{33}}A_l^2 \quad (7)$$

It is clearly seen that the dynamic CEMC K_{Dt} depends only on the speed V_{t5} of the corresponding bulk transverse wave. However, the dynamic CEMC K_{Dl} depends only on the speed V_l of the bulk longitudinal wave. Therefore, they can be called as transverse and longitudinal dynamic CEMCs, respectively. For dispersive waves, the V_{ph} depends on the layer thickness kh, and hence, the K_{Dt} and K_{Dl} will also depend on the kh. The K_{Dt} originates from its value of $K_0^2(C_{55} - 4C_{13})/C_{33}$ at $V_{ph} = 0$ and goes to its value of $-K_0^2(4C_{13} + 3C_{55})/C_{33}$ at $V_{ph} = V_{t5}$. On the other hand, the K_{Dl} has its maximum value of $K_0^2C_{11}/C_{33}$ at $V_{ph} = 0$ and equals to zero at $V_{ph} = V_l$. Both the dynamic CEMCs go to $-\infty$ with $V_{ph} \to +\infty$. Also, it is natural to note in Eq. (5) the following terms coupled with the cubic crystal anisotropy:

$$A_0 = \frac{C_{11}}{C_{33}}A_l^2 + A_t^2 + C^2 \qquad B_0 = \frac{C_{11}}{C_{33}}A_l^2A_t^2 \quad (8)$$

Figure 2 shows both the coefficients A_0 and B_0 as well as the K_{Dt} and K_{Dl} for the crystals $Bi_{12}SiO_{20}$, $Bi_{12}GeO_{20}$, and $Bi_{12}TiO_{20}$ in [110] propagation direction. Figure 2 clearly shows that values of the A_0 and B_0 can be one order greater than values of the K_{Dt} and K_{Dl}. It is noted that the anisotropy terms $C^2(Bi_{12}SiO_{20}) \sim 1.71$, $C^2(Bi_{12}GeO_{20}) \sim 1.55$, and $C^2(Bi_{12}TiO_{20}) \sim 1.75$ in [110] direction are significantly smaller than those in [100] direction, in which they represent the maximum possible C^2 of suitable propagation directions: $C^2(Bi_{12}SiO_{20}) \sim 2.55$, $C^2(Bi_{12}GeO_{20}) \sim 2.30$, and $C^2(Bi_{12}TiO_{20}) \sim 2.64$. Also, the threshold velocities V^{th} (Zakharenko, 2006) for the cubic crystals studied in Figure 2 are as follows: $V^{th}(Bi_{12}SiO_{20}) \sim 2826$ m/s, $V^{th}(Bi_{12}GeO_{20}) \sim 2795$ m/s, and $V^{th}(Bi_{12}TiO_{20}) \sim 2617$ m/s. For comparison, the threshold velocities V^{th} for (001) [100] direction are: $V^{th}(Bi_{12}SiO_{20}) \sim 3216$ m/s and $V^{th}(Bi_{12}GeO_{20}) \sim 3160$ m/s. Some piezoelectric acoustic crystals are listed in Table 2, in which the unique cubic crystals Tl_3TaS_4 and Tl_3TaSe_4 of the Chalcogenide family have very great values of C^2.

Using the crystal characteristics of Eqs. (7) and (8), Eq. (4) can be rewritten as follows:

$$m^3 + \left(A_0 + 1 - K_0^2\right)m^2 + \left(A_0 + B_0 + K_{Dt}\right)m + \left(B_0 + K_{Dl}\right) = 0 \quad (9)$$

After some transformations of Eq. (9), one can get the following equation

$$(m+1)\left(m^2 + A_0m - K_0^2m + B_0 + K_0^2 - K_{Dt}\right) + \left(K_{Dl} - K_{Dt} - K_0^2\right) = 0 \quad (10)$$

It is clearly seen in Eq. (10) that for a weak piezoelectrics $K_0^2 \to 0$ ($K_0^2 = 0$ and $K_{Dl} = K_{Dt} = 0$) there is

$$(m+1)\left(m^2 + A_0m + B_0\right) = 0 \quad (11)$$

The first factor in (11) represents equation corresponding to the pure electric potential wave:

$$n_3^{1,2} = \pm j \quad (12)$$

The second gives the following four roots:

$$n_3^{3,4,5,6} = \pm\left[-\frac{1}{2}A_0 \pm \frac{1}{2}\left(A_0^2 - 4B_0\right)^{1/2}\right]^{1/2} \quad (13)$$

which correlate with the roots of (Zakharenko, 2006) for (001) [110] propagation direction in non-piezoelectrics (Z-cut-X-direction in the crystallographic coordinate system).

Introducing the new function $y = m + A/3$, polynomial (4) can be rewritten to the following view $y^3 + 3py + 2q = 0$,

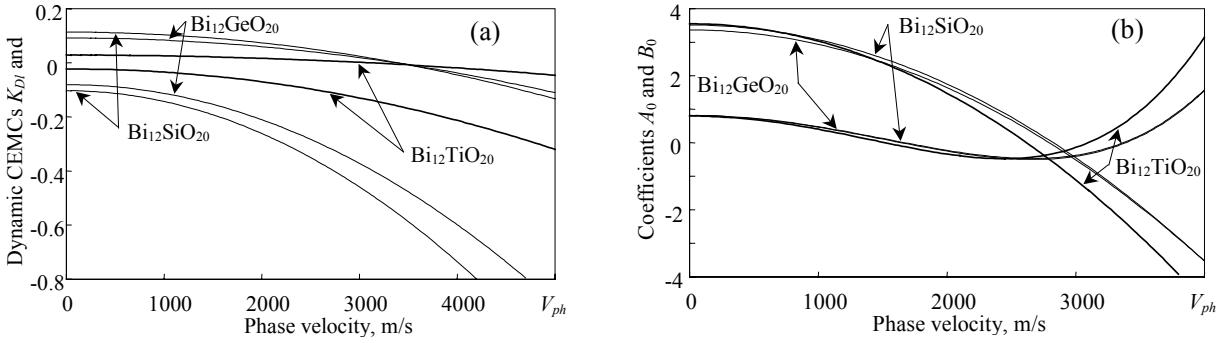

Fig. 2. The dynamic characteristics in [110] propagation direction for $Bi_{12}SiO_{20}$ (thin lines), $Bi_{12}GeO_{20}$ (normal), and $Bi_{12}TiO_{20}$ (thick): (a) K_{Dt} and K_{Dl} from Eq. (7), where there is $K_{Dl}(V_{ph} = V_l) = 0$ and $K_{Dt} < K_{Dl}$; (b) the coefficients A_0 and B_0 from Eq. (8), where there is $A_0(V_{ph} = V^{th}) = 0$ and $B_0(V_{ph} = V_t$ and $V_{ph} = V_l) = 0$.

for which the Cardano's formula can be applied, for instance, see the reference-book (Bronstein and Semendyaev, 2000). The coefficients q and p are defined as follows: $q = (A/3)^3 - (B/2)(A/3) + C/2$ and $p = B/3 - (A/3)^2$. Three roots $y_{1,2,3}$ depend on sign of the discriminant D, $D = q^2 + p^3$. If the D is negative due to $p < 0$, there are all three real roots. However, in the case of $D > 0$ there are one real and two imaginary roots. Also, if the coefficient C in (4) is positive, the real root is negative. It is clearly seen from (5) and (7) that the coefficient C can be positive both below the speed V_t and above the speed V_l. In addition, the coefficients A and B in (4) could be positive above the speed V_l for some cubic crystals with unique anisotropy properties, namely with a "gigantic" positive anisotropy term C^2 that was studied in (Zakharenko, 2006). It is noted that the anisotropy term C^2 can be both positive and negative, depending on the elastic constants. Therefore, there is a possibility to exist for the other type of surface waves polarized in the sagittal plane above the V_l, depending on both the crystal anisotropy and piezoelectric effect. For these waves, all complex/imaginary roots there are for polynomial (4). For the case of two real and four complex roots, there is also an existence possibility of in-plane polarized leaky waves with the $V_{ph} > V_t$.

Therefore, all six roots of polynomial (4) are as follows:

$$n_3^{1,2,3,4,5,6} = \pm\sqrt{-A/3 + y_{1,2,3}} \tag{14}$$

According to (Bronstein and Semendyaev, 2000), three roots $y_{1,2,3}$ are functions of values of w_1 and w_2, as well as of the roots $\alpha_{1,2} = -1/2 \pm j\sqrt{3}/2$ of the square equation $x^2 + x + 1 = 0$:

$$y_1 = w_1 + w_2 \quad y_2 = \alpha_1 w_1 + \alpha_2 w_2 \quad y_3 = \alpha_2 w_1 + \alpha_1 w_2 \tag{15}$$

where

$$w_1 = \sqrt[3]{-q + \sqrt{q^2 + p^3}} \quad w_2 = \sqrt[3]{-q - \sqrt{q^2 + p^3}} \tag{16}$$

It is noted that all three roots $y_{1,2,3}$ can be also found using the well-known Cardano's formula in the following view: $y_{1,2,3} = \xi - p/\xi$ with $\xi = [-q + \mathrm{sqrt}(q^2 + p^3)]^{1/3}$.

For each eigenvalue $n_3^{(N)}$ there is the corresponding so-called eigenvector ($U_1^{(N)}$, $U_3^{(N)}$, $\phi^{(N)}$):

$$U_1^{(N)} = +\left[C_{33}(n_3^{(N)})^2 + C_{55}A_t^2 + \frac{e_{15}^2}{\varepsilon_{11}}\frac{1}{1+(n_3^{(N)})^2}\right]^{1/2}$$

$$U_3^{(N)} = -\left[C_{55}(n_3^{(N)})^2 + C_{11}A_l^2 + 4\frac{e_{15}^2}{\varepsilon_{11}}\frac{(n_3^{(N)})^2}{1+(n_3^{(N)})^2}\right]^{1/2}$$

$$\phi^{(N)} = 2\frac{e_{15}}{\varepsilon_{11}}\frac{n_3^{(N)2}}{1+(n_3^{(N)})^2}U_1^{(N)} + \frac{e_{15}}{\varepsilon_{11}}\frac{1}{1+(n_3^{(N)})^2}U_3^{(N)} \tag{17}$$

In addition, the components $U_1^{(N)}$ and $U_3^{(N)}$ can be also found from the first equation in (2) as follows:

$$U_1^{(N)} = -(C_{13} + C_{55})n_3^{(N)} - 2C_{55}K_0^2\frac{n_3^{(N)}}{1+(n_3^{(N)})^2}$$

$$U_3^{(N)} = C_{55}(n_3^{(N)})^2 + C_{11}A_l^2 + 4C_{55}K_0^2\frac{(n_3^{(N)})^2}{1+(n_3^{(N)})^2}$$

which are equivalent, using Eq. (2). It is clearly seen in the latter equations that $U_1^{(N)}$ is imaginary, and $U_3^{(N)}$ is real depending on an imaginary $n_3^{(N)}$ that results in real $\phi^{(N)}$. On the other hand, $U_1^{(N)}$ and $U_3^{(N)}$ can be real and imaginary, respectively, resulting in imaginary $\phi^{(N)}$, if the second equation in (2) is treated. It is also noted that $U_1^{(N)}$ or $U_3^{(N)}$ can be chosen to be equal to unity for simplicity. The eigenvalues $n_3^{(N)}$ with negative imaginary part and the corresponding eigenvector components $u_1^{(N)} = U_1^{(N)}$, $u_3^{(N)} = U_3^{(N)}$, and $u_4^{(N)} = \phi^{(N)}$ are shown in Figure 3 for $Bi_{12}SiO_{20}$ and $Bi_{12}GeO_{20}$. Note that the $n_3^{(3)}$ is zero at $V_{ph} = V_t$.

All six eigenvalues $n_3^{(N)}$ in (14) must be taken for a layer, while only eigenvalues $n_3^{(N)}$ with negative imaginary part are left for a substrate, in order to have wave damping towards the depth of the substrate for the coordinate

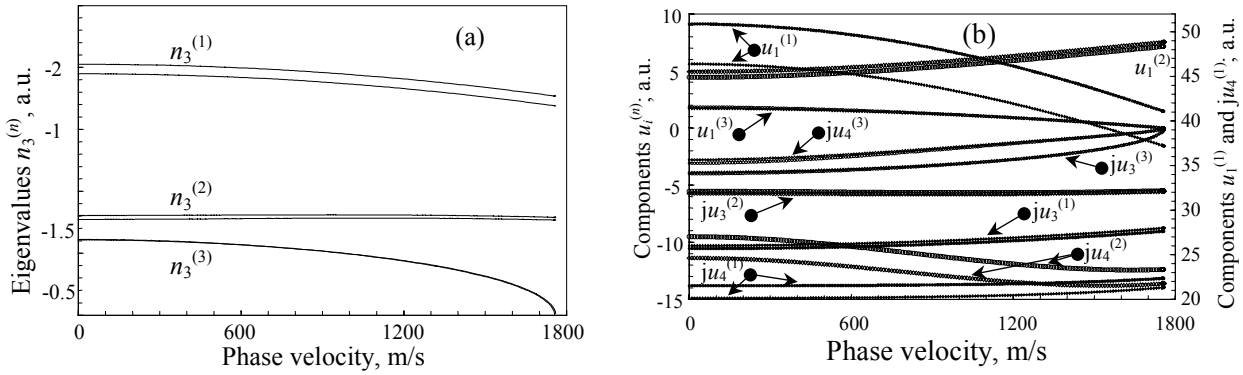

Fig. 3. (a) The eigenvalues $n_3^{(N)}$ for $Bi_{12}SiO_{20}$ (thin lines) and $Bi_{12}GeO_{20}$ (normal lines), where there is $n_3^{(1)} > n_3^{(2)} > n_3^{(3)}$; and (b) the eigenvector components $u_1^{(N)}$, $u_3^{(N)}$, and $u_4^{(N)} = \phi^{(N)}$ for $Bi_{12}SiO_{20}$ (cycles) and $Bi_{12}GeO_{20}$ (rhombs).

system shown in figure 1. Therefore, the complete mechanic displacements and the complete electric potential can be written as:

$$U_{1,3}^{\Sigma} = \sum_{N} F^{(N)} U_{1,3}^{(N)} \exp\left[\mathrm{j}\left(k_1 x_1 + k_3^{(N)} x_3 - \omega t\right)\right]$$

$$\phi^{\Sigma} = \sum_{N} F^{(N)} \phi^{(N)} \exp\left[\mathrm{j}\left(k_1 x_1 + k_3^{(N)} x_3 - \omega t\right)\right] \quad (18)$$

where $F^{(N)}$ are the so-called weight coefficients, and the index N runs from 1 to 3 for a substrate and from 1 to 6 for a layer.

For the free space, the Laplace's equation of type $\Delta\phi = 0$ is written in the following view: $\varepsilon_0(k_1^2 + k_3^2)\phi_0 = 0$, where ε_0 is the dielectric constant for the free space, $\varepsilon_0 = 8.854\times10^{-12}$ F/m. Because the wavevector component k_1 in the propagation direction is given the same in each medium (in a layer, a substrate and the free space), the electric potential for the free space is written as: $\phi_0 = F^{(0)}\exp(-k_1 x_3)\exp[\mathrm{j}(k_1 x_1 - \omega t)]$. The ϕ_0 should decrease with increase in the coordinate x_3. The V_{ph} of such Rayleigh-polarized waves should satisfy boundary conditions described in the next Section. Suitable V_{ph} of dispersive waves are found when the boundary conditions determinant equals to zero.

BOUNDARY CONDITIONS

Now both the complete mechanic displacements and the complete electric potential of Eq. (18) are substituted in the equations of mechanical and electrical boundary conditions based on the following requirements at both the interface of two solids (at $x_3 = 0$ in Fig. 1) and the free surface, $x_3 = h$:

1) continuity of the mechanic displacement U_1 at $x_3 = 0$ ($U_1^S = U_1^L$) where

$$U_1^S = \sum_{S(N)} F^{S(N)} U_1^{S(N)} \text{ and } U_1^L = \sum_{L(N)} F^{L(N)} U_1^{L(N)} \quad (19)$$

2) continuity of the mechanic displacement U_3 at $x_3 = 0$ ($U_3^S = U_3^L$) where

$$U_3^S = \sum_{S(N)} F^{S(N)} U_3^{S(N)} \text{ and } U_3^L = \sum_{L(N)} F^{L(N)} U_3^{L(N)} \quad (20)$$

3) continuity of the normal component ST_{31} of the stress tensor at $x_3 = 0$ ($\mathrm{ST}_{31}{}^S = \mathrm{ST}_{31}{}^L$) where

$$\mathrm{ST}_{31}^S = \sum_{S(N)} F^{S(N)}\left[C_{55}^S(k_3^{S(N)} U_1^{S(N)} + k_1 U_3^{S(N)}) + e_{15}^S k_1 \phi^{S(N)}\right]$$

$$\mathrm{ST}_{31}^L = \sum_{L(N)} F^{L(N)}\left[C_{55}^L(k_3^{L(N)} U_1^{L(N)} + k_1 U_3^{L(N)}) + e_{15}^L k_1 \phi^{L(N)}\right] \quad (21)$$

4) continuity of the normal component ST_{33} of the stress tensor at $x_3 = 0$ ($\mathrm{ST}_{33}{}^S = \mathrm{ST}_{33}{}^L$) where

$$\mathrm{ST}_{33}^S = \sum_{S(N)} F^{S(N)}\left[C_{13}^S k_1 U_1^{S(N)} + C_{33}^S k_3^{S(N)} U_3^{S(N)}\right]$$

$$\mathrm{ST}_{33}^L = \sum_{L(N)} F^{L(N)}\left[C_{13}^L k_1 U_1^{L(N)} + C_{33}^L k_3^{L(N)} U_3^{L(N)}\right] \quad (22)$$

5) continuity of the normal component D_3 of the electric displacements at $x_3 = 0$ ($D_3{}^S = D_3{}^L$) where

$$D_3^S = \sum_{S(N)} F^{S(N)}\left[e_{31}^S k_1 U_1^{S(N)} - \varepsilon_{33}^S k_3^{S(N)} \phi^{S(N)}\right]$$

$$D_3^L = \sum_{L(N)} F^{L(N)}\left[e_{31}^L k_1 U_1^{L(N)} - \varepsilon_{33}^L k_3^{L(N)} \phi^{L(N)}\right] \quad (23)$$

6) continuity of the electric potential ϕ at $x_3 = 0$ ($\phi^S = \phi^L$) where

$$\phi^S = \sum_{S(N)} F^{S(N)} \phi^{S(N)} \text{ and } \phi^L = \sum_{L(N)} F^{L(N)} \phi^{L(N)} \quad (24)$$

7) equality to zero of the stress tensor component: $\mathrm{ST}_{31}{}^L = 0$ at $x_3 = h$, where

$$\mathrm{ST}_{31}^L = \sum_{L(N)} F^{L(N)}\left[C_{55}^L(k_3^{L(N)} U_1^{L(N)} + k_1 U_3^{L(N)}) + e_{15}^L k_1 \phi^{L(N)}\right] \times \exp\left(\mathrm{j} k_3^{L(N)} h\right) \quad (25)$$

8) equality to zero of the stress tensor component: $\mathrm{ST}_{33}{}^L = 0$ at $x_3 = h$, where

$$\mathrm{ST}_{33}^L = \sum_{L(N)} F^{L(N)}\left[C_{13}^L k_1 U_1^{L(N)} + C_{33}^L k_3^{L(N)} U_3^{L(N)}\right] \times \exp\left(\mathrm{j} k_3^{L(N)} h\right) \quad (26)$$

9) continuity of the D_3 at $x_3 = h$ ($D_3{}^L = D_3{}^f$) where

$$D_3^L = \sum_{L(N)} F^{L(N)}\left[e_{31}^L k_1 U_1^{L(N)} - \varepsilon_{33}^L k_3^{L(N)} \phi^{L(N)}\right] \times \exp\left(\mathrm{j} k_3^{L(N)} h\right)$$

$$D_3^f = -F^{(0)} \phi_0^f \, \mathrm{j} k_1 \varepsilon_0 \exp\left(-k_1 h\right) \quad (27)$$

10) continuity of the electric potential ϕ at $x_3 = h$ ($\phi^L = \phi^f$) where

$$\phi^L = \sum_{L(N)} F^{L(N)} \phi^{L(N)} \exp\left(\mathrm{j} k_3^{L(N)} h\right) \text{ and}$$

$$\phi^f = F^{(0)} \phi_0^f \exp\left(-k_1 h\right) \quad (28)$$

In the boundary conditions (19)–(28), the indices L and S refer to quantities relative to the layer and substrate, respectively, $k_1^{L(N)} = k_1^{S(N)} = k_1 = k$. These equations form the equation set of ten homogeneous equations with unknown factors $F^{L(N)}$, $F^{S(N)}$, and $F^{(0)}$. Solutions for the V_{ph} can be numerically obtained when the tenth-order boundary conditions determinant (BCD10), consisting of coefficients at the unknown factors, becomes zero. It is noted that BCD10 can be readily reduced to BCD9 for finding the RTW9 phase velocity because values of the ϕ and D_3 can be taken to be not independent, for example, see (Farnell and Adler, 1972; Lardat *et al.*, 1971; Ingebrigtsen, 1969). Once ϕ is given, a fixed value D_3 is also given. Therefore, two boundary conditions (27) and (28) at the free surface can be written as single boundary condition for simplicity:

$$D_3 = \sum_{L(N)} F^{L(N)}\left[e_{31}^L k_1 U_1^{L(N)} - (\varepsilon_{33}^L k_3^{L(N)} - \mathrm{j} k_1 \varepsilon_0)\phi^{L(N)}\right] \times \exp\left(\mathrm{j} k_3^{L(N)} h\right) \quad (29)$$

To study the dispersive RTW9-waves is a complicated problem that can probably be solved numerically. It is noted that the boundary conditions (19)–(29) are changed for the so-called case of "shorted" surface. It is also noted that for weakly-piezoelectric materials there is $e_{15} \to 0$ ($e_{15} = 0$) that can result in appearance of two BCDs instead of BCD9 substituting $e_{15} = 0$ in Eq. (2). The first BCD6 of sixth-order gives the suitable V_{ph} for the non-

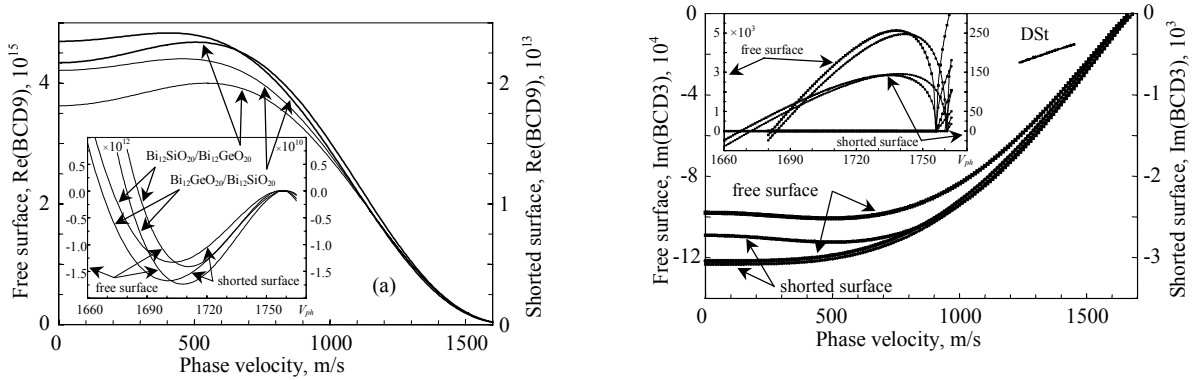

Fig. 4. The determinant behavior for (a) the RTW9-waves for the structures $Bi_{12}SiO_{20}/Bi_{12}GeO_{20}$ and $Bi_{12}GeO_{20}/Bi_{12}SiO_{20}$ with the free surface (thick lines, $kh \sim 1$) and the shorted surface (thin lines, $kh \sim 0.5$); and (b) the RTW3-waves for $Bi_{12}SiO_{20}$ (squares) and $Bi_{12}GeO_{20}$ (cycles), where "DSt" represents the determinant BCD6 for finding the Stoneley type waves.

piezoelectric RTW6-waves, and the second BCD corresponds to the electric potential wave. In this case, Eq. (4) goes into Eq. (11), which together with roots (12) and (13) give eigenvectors of the following view (0, 0, $\phi^{(N)}$) and ($U_1^{(N)}$, $U_3^{(N)}$, 0). Also, a BCD6 of sixth-order can be formed from the boundary conditions (19)–(29) for finding the V_{ph} of Rayleigh-polarized Stoneley type waves (STW6). However, such a BCD6 is not described in this Section to minimize the paper size, because non-dispersive waves propagating at the interface of two infinite solids were not found in the studied case.

Figure 4 shows behavior of determinants investigating both dispersive RTW9-waves and non-dispersive RTW3-waves. Real parts of the BCD9 for Rayleigh-polarized surface waves are given in Figure 4a in the V_{ph}-range: $0 < V_{ph} < V_t$. Both boundary conditions of free and shorted surfaces were studied for the layered system $Bi_{12}SiO_{20}/Bi_{12}GeO_{20}$ and the reverse configuration. The insertion in figure 4a shows solutions for the dispersive RTW9-waves, which are close to the corresponding speeds V_t for the crystals $Bi_{12}SiO_{20}$ and $Bi_{12}GeO_{20}$. Figure 4b shows the BCD3 imaginary parts for finding surface wave solutions in single crystals $Bi_{12}SiO_{20}$ and $Bi_{12}GeO_{20}$ for the V_{ph}-range using free and shorted surfaces. The insertion in figure 4b gives the solutions of surface RTW3-waves. For comparison, the BCD6 behavior for finding the Stoneley type waves, which could be localized at the interface between the crystals $Bi_{12}SiO_{20}$ and $Bi_{12}GeO_{20}$, is also shown in Figure 4b. It is noted that the absolute values of BCD9 for surface wave investigations in the studied structures are ten orders greater than those of BCD3 for the investigations in monocrystals that makes an additional difficulty to study layered systems.

NUMERICAL RESULTS AND DISCUSSIONS

In this paper, the numerical results are introduced concerning calculations of the V_{ph} of the dispersive RTW9-waves, accounting the piezoelectric effect for both the $Bi_{12}SiO_{20}$-layer and the $Bi_{12}GeO_{20}$-substrate in [110] direction for both media, in which the sagittal plane coincides with the symmetry plane of the media. For the numerical calculations, the elastic C_{ijkl}, piezoelectric e_{ijk}, and dielectric ε_{ij} material constants, and densities ρ of the treated media were taken from (Aleksandrov *et al*., 1984; Blistanov *et al*., 1982). Figure 5 shows the lowest-order modes of RTW9-waves (the so-called first type of the waves (Lardat *et al*., 1971)), namely dependence of the RTW9 phase velocity on the non-dimensional value of kh, where k is the wavenumber in the direction of wave propagation and h is the layer thickness. In general, the RTW9 lowest-order modes must be confined between the piezoelectric non-dispersive three-partial Rayleigh type wave (RTW3) for the $Bi_{12}GeO_{20}$-substrate at $kh \to 0$ and the wave for the $Bi_{12}SiO_{20}$-layer at $kh \to \infty$. However, that is not so at small kh in both studied layered systems for both cases of the free and shorted surfaces due to some peculiarities, which will be further discussed.

The dispersion relations in figures 5a (free surface) and 5b (metallized surface) show the existence possibility of non-dispersive Zakharenko type waves (ZTWs) after the work of Zakharenko (2005[a]). For the free surface, the nine-partial non-dispersive ZTW9-waves exist at $kh \sim 1.0$ in the both studied structures. However, for the metallized surface, they exists at $kh \sim 0.5$ showing a significant shift to smaller value of the kh. These non-dispersive ZTW9-waves split the corresponding RTW9 lowest-order mode into several sub-modes with different dispersion ($V_{ph} > V_g$ or $V_{ph} < V_g$, where V_g is the group velocity, $V_g = d\omega/dk$). Therefore, it is possible to state that each dispersive sub-mode starts with a non-dispersive wave and comes to a non-dispersive wave. There are two sub-modes for each case in figure 5. The RTW9 group velocity must have one extreme point in each sub-mode, because the behavior of the V_g depends on the behavior of the V_{ph}, $V_g = V_{ph} + kh(dV_{ph}/dkh)$, that was analytically shown in (Zakharenko, 2005[a]). It is obvious that increasing function $V_{ph}(kh)$ leads to the inequality $V_g > V_{ph}$ due to $dV_{ph}/dkh > 0$. On the

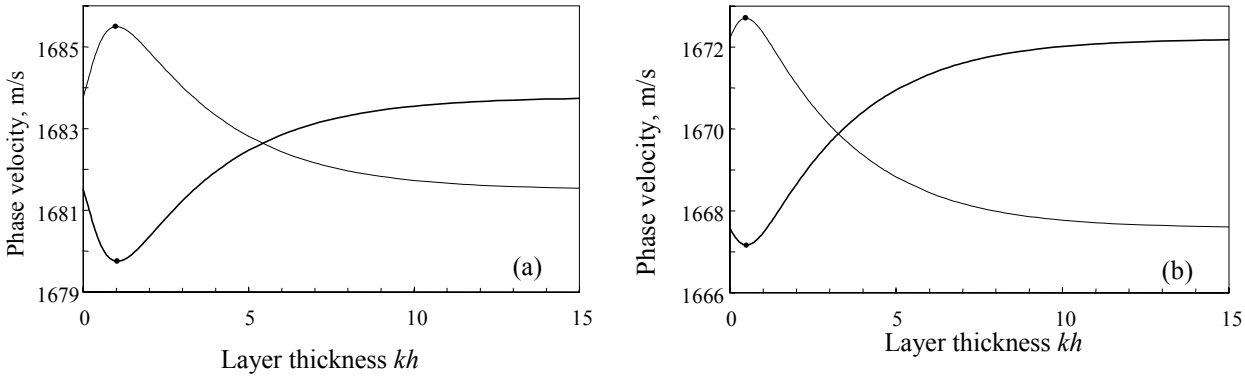

Fig. 5. The first type of dispersive RTW9-waves for the structures $Bi_{12}SiO_{20}/Bi_{12}GeO_{20}$ (thin lines) and $Bi_{12}GeO_{20}/Bi_{12}SiO_{20}$ (thick lines): a) for the free surface; b) for the metallized surface. The V_{ph} extreme points represent the non-dispersive ZTW9-waves.

other hand, decreasing $V_{ph}(kh)$ results in $V_g < V_{ph}$ because $dV_{ph}/dkh < 0$. The non-dispersive Zakharenko waves ($V_g = V_{ph} \neq 0$) existing in a mode of dispersive waves can be described by the following formulas, using the well-known Leibniz's formula for the complex derivative $d(u/v)/dx = (v du/dx - u dv/dx)/v^2$:

$$\frac{dV_{ph}}{dkh} = V_g \frac{dV_{ph}}{d\omega h} = 0 \tag{30}$$

$$\frac{dV_{ph}}{dkh} = \frac{1}{kh}\left(V_g - V_{ph}\right) \tag{31}$$

$$\frac{dV_{ph}}{d\omega h} = \frac{V_{ph}}{\omega h}\left(1 - \frac{V_{ph}}{V_g}\right) \tag{32}$$

The relationship (30) between the derivatives of V_{ph} shows that there is independence of the V_{ph} on both the angular frequency ω and the wavenumber k in the same k-ω-domain with $V_g \neq 0$. The formulas (31) and (32) give clearance that formula (30) is satisfied as soon as $V_{ph} = V_g$ for the wavenumber $k \neq 0$ and $k < \infty$. Note that the mass sensitivity of a sensor is generally defined as the relative velocity change due to the application of a thin non-elastic mass of thickness h_M and density ρ_M on top of a sensor surface. The normalized mass sensitivity can be also determined from the appropriate velocity dispersion (Jungnickel *et al*., 1997) because the sensitivity is proportional to the first derivative dV_{ph}/dkh_M. Note that the higher derivatives of the V_{ph} and V_g given in (Zakharenko, 2005[a]) can be also used to determine inflexion points (Zakharenko, 2005[b]).

The presence of the non-dispersive ZTW9-waves shown by points in figure 5 significantly broadens the V_{ph}-range of existence of the first type of dispersive RTW9-waves. The velocities V_{ph} of the RTW9 first type start with the corresponding non-dispersive RTW3-waves for the substrates at $kh = 0$ and approach the corresponding non-dispersive RTW3-waves at $kh \to +\infty$. It is noted that for the same layered systems, according to the numerical results of (Zakharenko, 2005[a]) concerning [100] direction, the first sub-mode of the lowest-order mode of the non-piezoelectric RTW6-waves at small values of kh lies out of the V_{ph}-range between the corresponding two non-dispersive RTW2-waves. The existence of the non-dispersive ZTW9-waves at small values of kh also occurs in several layered systems (Solie, 1971; Zhang *et al*., 2001). It is noted that the piezoelectric effect can significantly change the behavior of $V_{ph}(kh)$. Therefore, the electric potential ϕ must be considered together with dispositions of both the bulk longitudinal and corresponding transverse waves for materials in order to predict the existence possibility of non-dispersive ZTW-waves in different layered systems. For instance, for the studied layered systems (see Table 1) there are the following velocities: $V_L(Bi_{12}SiO_{20}) > V_L(Bi_{12}GeO_{20})$ and $V_{ST}(Bi_{12}SiO_{20}) < V_{ST}(Bi_{12}GeO_{20})$.

It is noted that the lowest-order modes for the studied layered systems are confined in a very narrow V_{ph}-range being smaller than ~ 6 ms^{-1} that can be convenient for some technical devices (Shiosaki *et al*., 1980). This can be compared with lowest-order modes of other suitable layered systems (Volyansky *et al*., 1987; Solie, 1971; Zhang *et al*., 2001) which are of interest for the same purpose. It is noted that experimental techniques are currently unknown by which it would be possible to make measurements of the V_{ph} with a precision at least 0.1 ms^{-1}. As of yet, the improved optical method for measurements of both the V_{ph} and V_g described in (Kolosovskii *et al*., 1998) allows one to measure the V_{ph} with an accuracy ~ 2 m/s. It may be possible to develop experimental technique for measurement of the derivative dV_{ph}/dkh (and/or $dV_{ph}/d\omega h$) together with the V_{ph}, in order to improve the measurement accuracy for weakly dispersive waves and to experimentally measure the non-dispersive ZTW-waves. It is noted that calculation accuracy of the V_{ph} in this work is about 10^{-3} m/s.

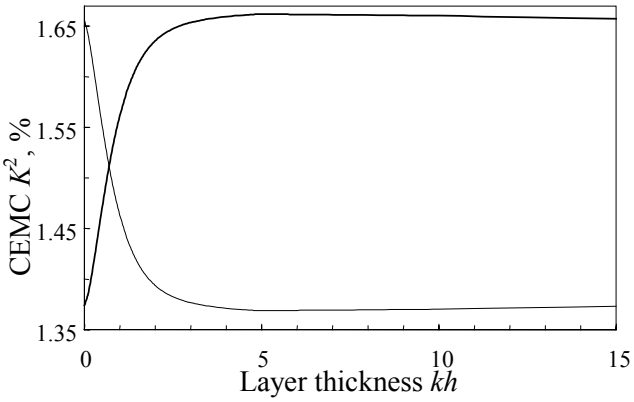

Fig. 6. The CEMCs K^2 (%) for the structures layer/substrate: $Bi_{12}SiO_{20}/Bi_{12}GeO_{20}$ (thick line) and $Bi_{12}GeO_{20}/Bi_{12}SiO_{20}$ (thin line).

The coefficient of the electromechanical coupling (CEMC) shown in figure 6 was calculated for the lowest-order modes of dispersive RTW9-waves with the following well-known formula:

$$K^2 = 2\frac{V_{Rf} - V_{Rm}}{V_{Rf}} \tag{33}$$

where V_{Rf} and V_{Rm} are the RTW9 phase velocities for the free and metallized surfaces, respectively. The CEMC K^2 is shown in figure 6 for both studied layered systems. For the structure $Bi_{12}SiO_{20}/Bi_{12}GeO_{20}$, the CEMC K^2 starts with the K^2 for the $Bi_{12}GeO_{20}$ single crystal at $kh = 0$ and approaches the K^2 for the $Bi_{12}SiO_{20}$ single crystal at $kh \rightarrow \infty$. It is noted that in the kh-range between ~ 3.3 and ~ 50, the CEMC $K^2(Bi_{12}SiO_{20}/Bi_{12}GeO_{20})$ is slightly larger than the $K^2(Bi_{12}SiO_{20}) \sim 0.016558$ with a maximum value at $kh \sim 5$. On the other hand, for the structure $Bi_{12}GeO_{20}/Bi_{12}SiO_{20}$, the CEMC K^2 starts with the $K^2(Bi_{12}SiO_{20})$ at $kh = 0$ and approaches the $K^2(Bi_{12}GeO_{20})$ at $kh \rightarrow \infty$. It is also noted that in the same kh-range, the CEMC $K^2(Bi_{12}GeO_{20}/Bi_{12}SiO_{20})$ is slightly smaller than the $K^2(Bi_{12}GeO_{20}) \sim 0.013742$ with a minimum value at approximately the same $kh \sim 5$. Therefore, using a hard piezoelectric layer on a softer piezoelectric substrate can result in increasing the CEMC K^2. In addition to the first type of dispersive RTW9-waves representing a single lowest-order mode, modes of the second type of RTW9-waves can exist in layered systems. They can exist if the speed V_t for a substrate is higher than that for a layer. This existence condition is full-filled for the structure $Bi_{12}SiO_{20}/Bi_{12}GeO_{20}$, but not for the structure $Bi_{12}GeO_{20}/Bi_{12}SiO_{20}$. The velocities $V_{ph}(kh)$ for seven modes of the RTW9 second type are shown in figure 7a. It is clearly seen in the figure that the first mode starts at $kh_0 \sim 43.2$, but not at $kh_0 = 0$. It was found that each next mode starts at $kh_\mu \sim kh_0 + 73\mu$, where μ is an integer number, $\mu = 1, 2, 3, \ldots$. In addition, it was verified that the neighbour kh_μ are equidistant from each other on the kh-scale. Figure 7b shows the BCD9 behaviour in the V_{ph}-range between the speeds V_t for the $Bi_{12}SiO_{20}$-layer and the $Bi_{12}GeO_{20}$-substrate for the RTW9 second type. It is clearly seen in figure 7b that the surface metallization does not change the V_{ph} that was verified at $kh = 500$ for the seven modes.

OTHER POSSIBILITIES FOR WAVE EXISTENCE

Ivanov and Kessenikh (1987) have assumed that in layered systems, consisting of a hard layer on a softer substrate both being the so-called transversely isotropic materials, Rayleigh-polarized dispersive waves such as slow surface waves can exist. These waves have a single mode starting with zero $V_{ph}(kh > 0)$ and approaching some non-dispersive velocity at $kh \rightarrow +\infty$ that they called Stoneley wave (SW). They have schematically shown that such slow surface mode could exist in the layered systems with $V_t^L > V_t^S > V_{R2}{}^S > V_{R2}{}^L > V_{St}$, where V_{St} represents the speed of the interfacial SW-wave, and V_t and V_{R2} are the speeds of the corresponding bulk transverse and surface RTW2 waves, respectively. However, it is thought that one of general features of a Stoneley wave is that it is faster than the slowest Rayleigh wave associated with the separated half-spaces (Destrade and Fu, 2006). Therefore, their representation of a dispersion branch originating from zero $V_{ph}(kh > 0)$ is a misconception. Hence, the problem on slow surface waves with the in-plane polarization is open concerning existence possibilities and specific conditions. The layered system $Bi_{12}GeO_{20}/Bi_{12}SiO_{20}$ studied in this paper possesses the following $V_t^L > V_t^S > V_{R3}{}^L > V_{R3}{}^S$, where V_{R3} is the surface RTW3-waves. Thus, STW-waves were not found in [110] direction. It is noted that such Rayleigh-polarized slow surface waves can be used for filter and sensor applications. For instance, there are Capacitive Micromachined Ultrasonic Transducers (CMUTs) of microelectromechanical system (MEMS) structures in integrated circuit (IC) technology (Yaralioglu *et al*., 2001). Generally, the CMUTs are based on the Rayleigh-polarized Lamb waves (flexural plate mode) and could be also manufactured on the Love-wave polarized slow surface Zakharenko waves (SSZWs) recently introduced in (Zakharenko, 2005[b]).

Also, note that the other possibility of wave existence in addition to dispersive RTW-waves is the existence of non-dispersive Zakharenko type waves in different layered structures. However, the non-dispersive ZTW-waves were introduced as dispersive waves in all papers concerning investigations of dispersive waves. In addition, there are works in which there are attempts to represent results concerning dispersive waves with a very weak dependence $V_{ph}(kh)$ as non-dispersive waves, for example (Cherednik and Dvoesherstov, 2003; Dvoesherstov *et al*., 2003). That is somewhat incorrect from the view point shown in this paper. It is noted that if one will draw phase velocities of dispersive electro-magnetic (EMW) and acoustic (AW) waves on the same

scale, one will find that the AWs become non-dispersive compared with the dispersive EM-waves, because the EM-waves are characterized by the V_{ph} being five orders higher than that of the AWs. It is also noted that the AW highest speed is ~ 20000 ms^{-1} for Diamond and some non-cubic crystals (Zakharenko, 2005[b]).

It was also assumed that there is an existence possibility to find Rayleigh-polarized supersonic surface waves in both monocrystals and layered systems. The V_{ph} of such supersonic surface waves will be higher than the speed V_t. The supersonic surface waves could exist in monocrystals with a great C^2 accounting possible effects: piezoelectric, piezomagnetic, etc. Some possible effects are shown in (Aboudi, 2000; Bednarcyk, 2002). The values of C^2 calculated in Section 3 for the studied monocrystals are not great. However, the coefficients A_0 and B_0 are relatively the same slightly above the corresponding speeds V_l up to 4000 m/s that is seen from figure 2b. The absolute values of the K_{Dl} and K_{Dt} are one order smaller than that of the A_0 and B_0 shown in figure 2a. It is noted that the coefficients A, B, and C in Eq. (5) should be all positive, in order to give two complex/imaginary roots plus one negative real root of the third order polynomial in (4) for surface waves. However, for surface waves, it is possible to have such the polynomial roots for Abs(A) ~ Abs(B) ~ Abs(C) with the coefficient A or B being negative. It is difficult to find such crystals because the K_{Dt} is negative for $V_{ph} > V_t$ giving negative B. Therefore, a computer program is given in the Appendix. Indeed, it is possible to treat crystals accounting other suitable effects in addition to piezoelectric/piezomagnetic effect. For instance, if the A, B, and C in Eq. (5) give the following polynomial $P_3 = x^3 + 0.5x^2 - 0.1x + 0.01$, the corresponding two complex and one negative real root solving the equation $P_3 = 0$ will be as follows: {– 0.6712; 0.0856 – I0.0870; 0.0856 + I0.0870}. That results in appearance of four complex and two imaginary roots for the sixth order polynomial in Eq. (4) with $m = n_3^2$, three of which with negative imaginary part are suitable for surface wave existence: {– I0.8193; 0.3222 – I0.1350; – 0.3222 – I0.1350} with I = $(-1)^{1/2}$. Indeed, such situation is possible showing instability of some piezoelectric (piezomagnetic, etc.) crystals about the velocity V_l. That can happen in a very narrow V_{ph}-range with a very small C in Eq. (4). For example, the following polynomial $P_3 = x^3 + x^2 - 0.01x + 0.0001$ has its roots solving equation $P_3 = 0$: {– 1.009999; 0.0045 – I0.0086; 0.0045 + I0.0086}. That gives the following suitable roots of the sixth order polynomial {– I1.0050; 0.0865 – I0.0498; – 0.0865 – I0.0498} for SAW existence.

Finally, it is noted that modes of dispersive leaky Sezawa type waves with the in-plane polarization can exist for $V_{ph} > V_t$ looking like corresponding continuations of the modes of dispersive RTW9 second type shown in figure 7a. Solutions for such ultrasonic leaky waves were not found with $V_{ph} > V_t$ by evaluating the BCD9 sign running up to the speed V_l, at which the complex BCD9 becomes zero. Probably, they are found above the speed V_t when minima of Abs (BCD9) are treated instead of monitoring changes in sign of the corresponding BCD9 part, because it is thought that the latter is preferable for finding SAWs.

PURE RTW9-WAVES IN 20^0-x_2-ROTATED DIRECTION

This Section studies pure RTW9-wave propagation in layered systems, consisting of cubic crystals $Bi_{12}SiO_{20}$ and $Bi_{12}GeO_{20}$ accounting the piezoelectric effect. The waves propagate in the so-called work coordinate system obtained from [110] direction by 20^0-rotation around the x_2-axis in figure 1 for both materials. In this propagation direction there are the following non-zero material constants: the elastic constants C_{11}, C_{33}, C_{13}, C_{55}, C_{15} with negative C_{35}, the piezoelectric constants e_{13}, e_{31}, e_{33}, e_{15}, e_{35} with negative e_{11}. They correspond to the complicated case of monoclinic crystals. The dielectric constants do not changed, $\varepsilon_{11} = \varepsilon_{33}$ with $\varepsilon_{13} = 0$. Therefore, the theory developed in the second and third Sections is not suitable

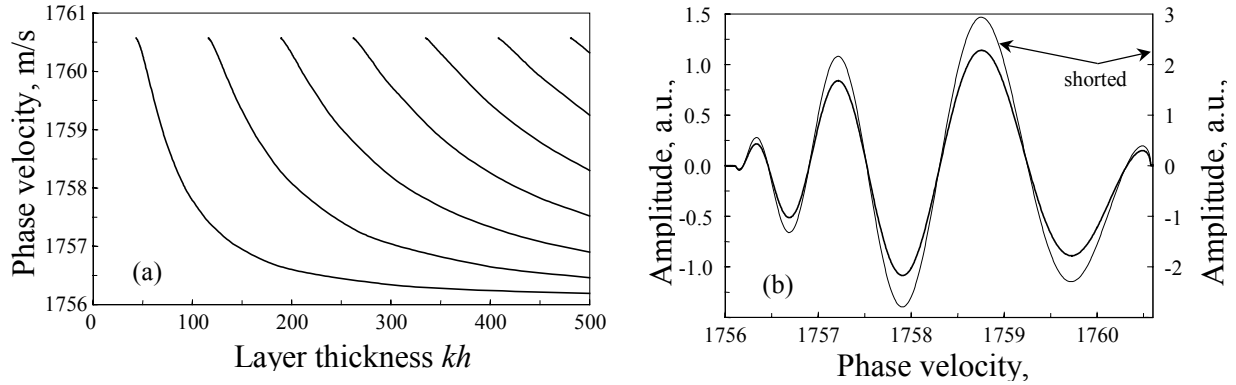

Fig. 7. For the structure $Bi_{12}SiO_{20}/Bi_{12}GeO_{20}$: (a) the seven modes of dispersive RTW9 second type; and (b) the corresponding BCD9 behavior at the layer thickness kh = 500 for the free (thick line) and metallized (thin line) surfaces.

here and there is only numerical analysis as a studying instrument. Figure 8a shows existence of the RTW9 first type for two different electrical boundary conditions: the free and metallized surface. The boundary conditions allow evaluation of the CEMC K^2 (%) shown in Figure 8b. It is clearly seen in the Figure that the CEMC is not larger than 1.5% for both studied structures: $Bi_{12}SiO_{20}/Bi_{12}GeO_{20}$ and the reverse configuration. Indeed, the CEMC starts at its value for the corresponding substrate at $kh \rightarrow 0$ and approaches its value for the corresponding layer at $kh \rightarrow \infty$ in the both cases. It is clearly seen in figure 8a that the first type of dispersive RTW9-waves possesses one non-dispersive Zakharenko type wave (ZTW9) at $kh \sim 1.39$ to 1.40 for the free surface and two for the metallized surface at $kh \sim 0.13$ to 0.15 and at $kh \sim 1.15$ to 1.18. The insertion in Figure 8b shows the first non-dispersive ZTW9-wave at small kh for the shorted case.

The dispersion relations for the structures $Bi_{12}SiO_{20}/Bi_{12}GeO_{20}$ and $Bi_{12}GeO_{20}/Bi_{12}SiO_{20}$ look like mirror reflections of each other. However, that is not completely true for both electrical boundary conditions. For instance, there is kh-position of the non-dispersive ZTW9-wave at $kh \sim 1.39$ for the structure $Bi_{12}SiO_{20}/Bi_{12}GeO_{20}$ and at $kh \sim 1.40$ for the structure $Bi_{12}GeO_{20}/Bi_{12}SiO_{20}$ that shows small asymmetry of the systems. A small asymmetry there is also for the shorted case. It is noted that calculation accuracy for finding the V_{ph} was possible to set at 1μm/sec. However, it is thought that it is necessary to take a trustable V_{ph}-accuracy about 1mm/sec. Therefore, it is possible to trust that the presence of the non-dispersive ZTW9-wave in both structures at small $kh \sim 0.13$ to 0.15 shown in the insertion is true. It is obvious that the existence of the non-dispersive ZTW9-waves at the small kh for the shorted case is caused by only piezoelectric properties, because they do not exist when the surface is free of metallization. On the other hand, the presence of the non-dispersive ZTW9-waves at larger $kh \sim 1.0$ to 1.5 for both the cases is caused by both the elastic and piezoelectric material properties. It is thought that here the elastic properties play a major role. "Shortage" of the free surface results in significant change in the kh-position of the corresponding non-dispersive ZTW9-wave, namely there is a shift to smaller values of kh showing the piezoelectricity influence. Also, it is obvious that the presence of the non-dispersive ZTW9-waves broadens the V_{ph}-existence range of the dispersive RTW9-waves. Indeed, the V_{ph}-range for the RTW9-waves' localization is about three times greater than the initially given V_{ph}-difference of $V_{RTW3}(Bi_{12}GeO_{20})$ = 1734.674 m/s from $V_{RTW3}(Bi_{12}SiO_{20})$ = 1733.631 m/s (see the third column in Table 3). The RTW3 phase velocities with the metallized surface are as follows: $V_{RTW3m}(Bi_{12}GeO_{20})$ = 1723.997 m/s and $V_{RTW3m}(Bi_{12}SiO_{20})$ = 1720.775 m/s.

According to table 3, the RTW9 second type could exist in the layered system, consisting of the $Bi_{12}GeO_{20}$-layer on the $Bi_{12}SiO_{20}$-substrate, because for the slow transverse waves there is $V_{ST}(Bi_{12}SiO_{20}) > V_{ST}(Bi_{12}GeO_{20})$ representing the condition for the wave existence. The condition is true studying wave propagation in isotropic media as well as in many suitable propagation directions in anisotropic and piezoelectric materials. However, the existence of RTW9 second type does not obey the condition in the propagation direction studied in this Section. The waves exist in the reverse configuration, because it is necessary to treat the so-called velocity equivalent V_{ph0} listed in the last column of table 3. The velocity V_{ph0} corresponds to the case when imaginary part of one root with the smallest imaginary part disappears. That occurs for $V_{ph0}(Bi_{12}GeO_{20})$ = 1829.135307 m/s giving m_3 = 0.217658 – I5.65406E–06 and $V_{ph0}(Bi_{12}SiO_{20})$ = 1825.255744 m/s with m_3 = 0.220269 – I1.81874E–05, where I = $(-1)^{1/2}$. Therefore, the existence condition of the RTW9 second type is $V_{ph0}(Bi_{12}GeO_{20}) > V_{ph0}(Bi_{12}SiO_{20})$ instead of $V_{ST}(Bi_{12}SiO_{20}) > V_{ST}(Bi_{12}GeO_{20})$. That is an additional difficulty for finding the RTW9 second type. Several modes of the dispersive RTW9 second type are shown in figure 9 within relatively great kh-range: $0 < kh < 500$. The first mode begins at

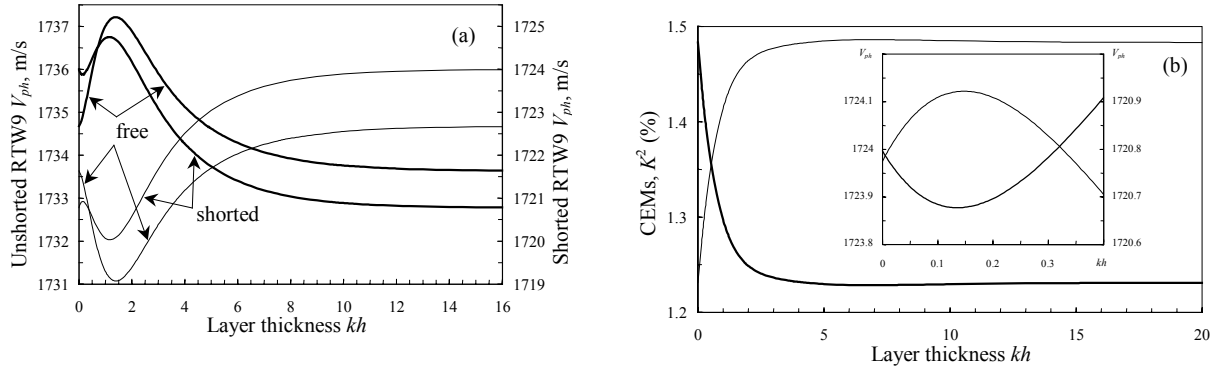

Fig. 8. (a) The dependence $V_{ph}(kh)$ for the RTW9 first type: the thick lines are for the structure $Bi_{12}SiO_{20}/Bi_{12}GeO_{20}$ and the thin lines are for the structure $Bi_{12}GeO_{20}/Bi_{12}SiO_{20}$; (b) the coefficient K^2 (%) with the insertion showing $V_{ph}(kh)$ at small kh.

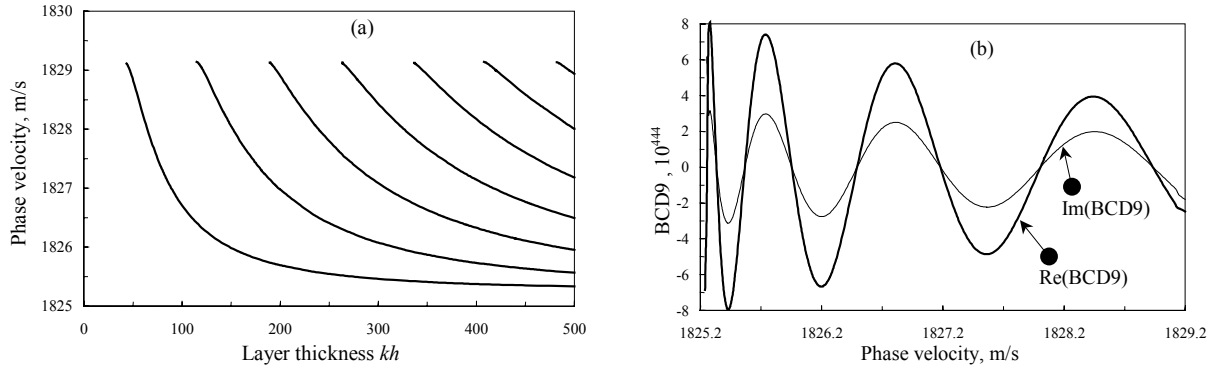

Fig. 9. (a) Several modes of the RTW9 second type for the structure $Bi_{12}SiO_{20}/Bi_{12}GeO_{20}$; (b) the corresponding complex BCD9 for the layer thickness $kh = 500$.

quite great values of $kh \sim 43.5$. Each next mode beginning looks like to be equidistant from the previous with the kh-step ~ 72 to 74. Figure 9b shows the sinusoidal behavior of both the real and imaginary parts of the complex BCD9.

It was found that both the boundary condition determinants BCD3 and BCD9 do not equal to zero at the corresponding bulk wave speeds V_{ST} listed in table 3. At the speed V_{ST} there is the following: one corresponding positive real root in addition to two complex roots with negative imaginary part changes its sign. It is noted that the velocity V_{ph0} is a common feature that appears not only studying pure RTW9-waves, but also studying pure Love type waves (LTWs) with the anisotropy factor $\alpha_f = (C_{44}C_{66} - C_{46}^2)^{1/2}/C_{44}$ (Lardat *et al*., 1971; Zakharenko, 2005[b]). The LTW velocity equivalent β should be lower than the speed V_{FT} of the corresponding shear (fast transverse) bulk wave, $V_{FT} = \left(C_{66}/\rho\right)^{1/2}$, due to the condition $C_{66}C_{44} > C_{46}^2$ requiring for energy conservation (Lardat *et al*., 1971). That may also be true for RTW9-waves giving $V_{ph0} < V_{ST}$. Here there is $C_{46} \neq 0$ for the 20^0-x_2-rotation from [110] direction. It is noted that there are the following waves: $V_{FT}(Bi_{12}SiO_{20}) = 2274.364$ m/s and $V_{FT}(Bi_{12}GeO_{20}) = 2255.092$ m/s giving higher V_{ph} of Love type waves compared with V_{ST} listed in Table 3 for RTW3-waves. The studied propagation direction is one of possible cuts using the x_2-rotation from ~ 19^0 up to ~ 30^0 with the condition $V^L_{ST} > V^S_{ST} > V^S_{RTW3} > V^L_{RTW3}$.

Solutions above the speed V_{ST} were also found. It was found that the complex BCD3 equals to zero at $V_{ph1} \sim$ 1963.492 m/s studying wave existence in the monocrystal of $Bi_{12}GeO_{20}$. That happens when the negative real root of three roots $\{m_3^{(1)} = -0.644149 - I1.11408;\ m_3^{(2)} = 0.09105 - I0.818141;\ m_3^{(3)} = -0.0490123\}$ gives all zero components ($U_1^{(3)}$, $U_3^{(3)}$, $\phi^{(3)}$). It is noted that the zero components give the following weight factors $\{F^{(1)}; F^{(2)}; F^{(3)}\} = \{0; 0; F^{(3)}\}$ or $\{0; 0; 0\}$ in the complete characteristics $U_{1,3,4} = \sum_{N=1,2,3} F^{(N)} U^{(N)}_{1,3,4} \exp\left[jk\left(m_1 x_1 + m_3^{(N)} x_3 - \omega t\right)\right]$ with $U_4^{(N)} = \phi^{(N)}$ manifesting that such waves cannot exist. However, if suitable weight factors $\{F^{(1)}; F^{(2)}; 0\}$ will be found that is an additional investigation problem, it is possible to study two-partial waves instead of three-partial waves concerning wave propagation in monocrystals. As soon as the BCD3 equals to zero at V_{ph1}, the complex BCD9 for structures using any layer on the substrate, as well as all corresponding higher-order BCDs studying multi-layered structures, will be zero at the same V_{ph1} due to the zero components ($U_1^{(3)}$, $U_3^{(3)}$, $\phi^{(3)}$) for the substrate. The same there is for $Bi_{12}SiO_{20}$ and layered structures with the substrate of $Bi_{12}SiO_{20}$, where all zero components ($U_1^{(3)}$, $U_3^{(3)}$, $\phi^{(3)}$) are for the roots $\{m_3^{(1)} = -0.700865 - I1.13238;\ m_3^{(2)} = 0.105407 - I0.800113;\ m_3^{(3)} = -0.048674\}$ at $V_{ph1} \sim 1965.258$ m/s. It is noted that the speeds V_L of the longitudinal bulk wave for the 20^0-x_2-rotated direction are as follows: $V_L(Bi_{12}SiO_{20}) = 3359.358$ m/s and $V_L(Bi_{12}GeO_{20}) = 3337.419$ m/s. However, the second pair of complex roots disappears at a velocity equivalent V_{ph2}, which is lower than the speed V_L. For example, there is $V_{ph2}(Bi_{12}SiO_{20}) \sim 3355.468$ m/s. Probably, such the situation when the speeds V_{ST} and V_L do not coincide with the corresponding velocity equivalents V_{ph0} and V_{ph2} is common.

CONCLUSIONS

In this theoretical work, the possible existence of supersonic surface waves with the Rayleigh-wave polarization is shown. For these waves, the phase velocity V_{ph} could be found about the speed V_l depending on both the crystal anisotropy and the piezoelectric/piezomagnetic effect. The computer program is given in the Appendix, which can be used for finding the supersonic waves in addition to the RTW3 and RTW9-waves. Note that many crystals can possess both effects, according to Al'shits and Lyubimov (1990), as well as the other effects, see (Aboudi, 2000; Bednarcyk, 2002). That can significantly complicate calculations in numerical experiments. Also, both the longitudinal dynamic CEMC $K_{Dl}(V_l)$ and the

transverse dynamic CEMC $K_{Dt}(V_{t5})$ were introduced and discussed. Possible existence of slow surface waves with the Rayleigh-wave polarization was also discussed. The introduced calculations of the RTW9 lowest-order mode in the layered system, consisting of the materials $Bi_{12}SiO_{20}$ and $Bi_{12}GeO_{20}$, have shown the existence of the non-dispersive Zakharenko type waves (ZTW9) in the studied layered systems with both the free surface and surface metallization. It was found that the surface metallization can significantly shift the appearance of the non-dispersive ZTW9-waves to smaller values of *kh*. It was also found that at $kh \sim 5 - 6$ the CEMC K^2 for the structure $Bi_{12}GeO_{20}/Bi_{12}SiO_{20}$ is slightly larger than that for the $Bi_{12}GeO_{20}$ single crystal. The non-dispersive ZTW9-waves divide the RTW9 lowest-order mode into sub-modes with different dispersions, $V_{ph} > V_g$ or $V_{ph} < V_g$. This lowest-order mode of dispersive RTW9-waves is confined in the narrow V_{ph}-range between the non-dispersive RTW3-wave for the $Bi_{12}SiO_{20}$-layer and the wave for the $Bi_{12}GeO_{20}$-substrate. That can be convenient for some technical devices, for which a weak dependence of the V_{ph} on the layer thickness *kh* is required. For comparison, the 20^0-x_2-rotated propagation direction from [110] direction was also studied concerning the pure RTW9-waves. Here, it was found that existence of RTW9 second type does not depend on the speeds V_t of the corresponding bulk transverse waves in both materials.

ACKNOWLEDGEMENTS

I thank Dr. Victor Y. Zhang for useful notes and his paper sent to me.

Appendix. The Maple program for finding the phase velocity of the RTW3 and RTW9-waves:

```
restart: with(linalg): ms:=array(1..3,1..3):
ms1:=array(1..3,1..3): u1s:=array(1..6): u3s:=array(1..6):
u4s:=array(1..6): m3s:=array(1..6): c33s:=12.962:
c13s:=2.985: c55s:=2.451: c11s:=c55s+(c13s+c33s)/2:
c66s:=4.9885: ros:=9.07: es:=1.122: dps:=3.63735:
dp0:=0.08854: fdz:=fopen("RTW9_1.txt",WRITE):
c2s:=(c11s*c33s-c55s*(c11s+c33s)+c55s^2-
(c13s+c55s)^2)/(c33s*c55s); k0s:=es*es/(c55s*dps):
Vt5s:=1000*sqrt(10*c55s/ros);
Vt6s:=1000*sqrt(10*c66s/ros);
Vls:=1000*sqrt(10*c11s/ros);
Vts_new:=Vt5s*sqrt(1+k0s); mg:=array(1..3,1..3):
mg1:=array(1..3,1..3): u1g:=array(1..6): u3g:=array(1..6):
u4g:=array(1..6): m3g:=array(1..6): c33g:=12.852:
c13g:=2.934: c55g:=2.562: c11g:=c55g+(c13g+c33g)/2:
dp0:=0.08854: c2g:=(c11g*c33g-
c55g*(c11g+c33g)+c55g^2-
(c13g+c55g)^2)/(c33g*c55g); rog:=9.2: dpg:=3.336:
eg:=0.983: k0g:=eg*eg/(c55g*dpg):
Vt5g:=1000*sqrt(10*c55g/rog);
Vlg:=1000*sqrt(10*c11g/rog);
Vtg_new:=Vt5g*sqrt(1+k0g); st66:=array(1..6,1..6);
rw9:=array(1..9,1..9): for kh from 0 by 0.1 to 10 do
Drw9:=0: for i from 1675 by 0.1 to 1685 do  Vph:=i:
At2s:=1-(Vph/Vt5s)^2: Al2s:=1-(Vph/Vls)^2:
B0s:=(c11s/c33s)*At2s*Al2s:
A0s:=(c11s/c33s)*Al2s+At2s+c2s:
kdts:=k0s*(4*c55s*At2s-4*c13s-3*c55s)/c33s:
kdls:=k0s*c11s*Al2s/c33s: As:=A0s+1+4*k0s:
Bs:=A0s+B0s+kdts: Cs:=B0s+kdls:
Pls:=ns^3+As*ns^2+Bs*ns+Cs: sols:=[solve(Pls,ns)]:
At2g:=1-(Vph/Vt5g)^2: Al2g:=1-(Vph/Vlg)^2:
B0g:=(c11g/c33g)*At2g*Al2g;
A0g:=(c11g/c33g)*Al2g+At2g+c2g;
kdtg:=k0g*(4*c55g*At2g-4*c13g-3*c55g)/c33g;
kdlg:=k0g*c11g*Al2g/c33g; Ag:=A0g+1+4*k0g:
Bg:=A0g+B0g+kdtg: Cg:=B0g+kdlg:
Plg:=ng^3+Ag*ng^2+Bg*ng+Cg: solg:=[solve(Plg,ng)]:
for j from 1 by 1 to 3 do   m3s[j]:=-sqrt(sols[j]): m3g[j]:=-
sqrt(solg[j]):  m3s[3+j]:=sqrt(sols[j]):
m3g[3+j]:=sqrt(solg[j]):   u1s[j]:=-
(es^2/dps)*(1/(1+m3s[j]^2))-(c33s*m3s[j]^2+c55s*At2s):
u3s[j]:=(c13s+c55s)*m3s[j]+(2*es^2/dps)*(m3s[j]/(1+m3
s[j]^2)):
u4s[j]:=(2*es/dps)*(m3s[j]/(1+m3s[j]^2))*u1s[j]+(es/dps)
*(1/(1+m3s[j]^2))*u3s[j]:
u1s[3+j]:=-(es^2/dps)*(1/(1+m3s[3+j]^2))-
(c33s*m3s[3+j]^2+c55s*At2s):
u3s[3+j]:=(c13s+c55s)*m3s[3+j]+(2*es^2/dps)*(m3s[3+j
]/(1+m3s[3+j]^2)):
u4s[3+j]:=(2*es/dps)*(m3s[3+j]/(1+m3s[3+j]^2))*u1s[3+
j]+(es/dps)*(1/(1+m3s[3+j]^2))*u3s[3+j]:
u1g[j]:=-(eg^2/dpg)*(1/(1+m3g[j]^2))-
(c33g*m3g[j]^2+c55g*At2g):
u3g[j]:=(c13g+c55g)*m3g[j]+(2*eg^2/dpg)*(m3g[j]/(1+
m3g[j]^2)):
u4g[j]:=(2*eg/dpg)*(m3g[j]/(1+m3g[j]^2))*u1g[j]+(eg/dp
g)*(1/(1+m3g[j]^2))*u3g[j]:
u1g[3+j]:=-(eg^2/dpg)*(1/(1+m3g[3+j]^2))-
(c33g*m3g[3+j]^2+c55g*At2g):
u3g[3+j]:=(c13g+c55g)*m3g[3+j]+(2*eg^2/dpg)*(m3g[3
+j]/(1+m3g[3+j]^2)):
u4g[3+j]:=(2*eg/dpg)*(m3g[3+j]/(1+m3g[3+j]^2))*u1g[3
+j]+(eg/dpg)*(1/(1+m3g[3+j]^2))*u3g[3+j]:
ms[1,j]:=c55s*(m3s[j]*u1s[j]+u3s[j])+es*u4s[j]:
ms[2,j]:=c13s*u1s[j]+m3s[j]*c33s*u3s[j]:
ms[3,j]:=es*u1s[j]-(dps*m3s[j]-dp0*I)*u4s[j]:
ms1[1,j]:=c55s*(m3s[3+j]*u1s[3+j]+u3s[3+j])+es*u4s[3
+j]:
ms1[2,j]:=c13s*u1s[3+j]+m3s[3+j]*c33s*u3s[3+j]:ms1[3
,j]:=es*u1s[3+j]-(dps*m3s[3+j]-dp0*I)*u4s[3+j]:
mg[1,j]:=c55g*(m3g[j]*u1g[j]+u3g[j])+eg*u4g[j]:
mg[2,j]:=c13g*u1g[j]+m3g[j]*c33g*u3g[j]:
mg[3,j]:=eg*u1g[j]-(dpg*m3g[j]-dp0*I)*u4g[j]:
mg1[1,j]:=c55g*(m3g[3+j]*u1g[3+j]+u3g[3+j])+eg*u4g[
3+j]:
mg1[2,j]:=c13g*u1g[3+j]+m3g[3+j]*c33g*u3g[3+j]:mg1
[3,j]:=eg*u1g[3+j]-(dpg*m3g[3+j]-dp0*I)*u4g[3+j]:
```

```
rw9[1,j]:=u1s[j]: rw9[1,3+j]:=-u1g[j]: rw9[1,6+j]:=-
u1g[3+j]: rw9[2,j]:=u3s[j]: rw9[2,3+j]:=-u3g[j]:
rw9[2,6+j]:=-u3g[3+j]: rw9[3,j]:=u4s[j]: rw9[3,3+j]:=-
u4g[j]: rw9[3,6+j]:=-u4g[3+j]: rw9[4,j]:=ms[1,j]:
rw9[4,3+j]:=-mg[1,j]: rw9[4,6+j]:=-mg1[1,j]:
rw9[5,j]:=ms[2,j]: rw9[5,3+j]:=-mg[2,j]: rw9[5,6+j]:=-
mg1[2,j]: rw9[6,j]:=ms[3,j]-dp0*I*u4s[j]: rw9[6,3+j]:=-
(mg[3,j]-dp0*I*u4g[j]): rw9[6,6+j]:=-(mg1[3,j]-
dp0*I*u4g[3+j]): rw9[7,j]:=0: rw9[8,j]:=0: rw9[9,j]:=0:
rw9[7,3+j]:=mg[1,j]*exp(I*kh*m3g[j]):
rw9[7,6+j]:=mg1[1,j]*exp(I*kh*m3g[3+j]):
rw9[8,3+j]:=mg[2,j]*exp(I*kh*m3g[j]):
rw9[8,6+j]:=mg1[2,j]*exp(I*kh*m3g[3+j]):
rw9[9,3+j]:=mg[3,j]*exp(I*kh*m3g[j]):
rw9[9,6+j]:=mg1[3,j]*exp(I*kh*m3g[3+j]): end do:
Ds:=det(ms): Dg:=det(mg):
ADs:=sqrt(Re(Ds)^2+Im(Ds)^2):
ADg:=sqrt(Re(Dg)^2+Im(Dg)^2): Drw91:=Drw9:
Drw9:=det(rw9):
ADrw9:=sqrt(Re(Drw9)^2+Im(Drw9)^2):
if (Drw9*Drw91<0) then  fprintf(fdz,"kh %g  Vph %g
Re(Ds) %g  Im(Ds) %g  ADs %g   Re(Dg) %g  Im(Dg)
%g  ADg %g   Re(Drw9) %g  Im(Drw9) %g  ADrw9
%g",kh,Vph,Re(Ds),Im(Ds),ADs,Re(Dg),Im(Dg),ADg,
Re(Drw9),Im(Drw9),ADrw9):   end if: end do: end do:
fclose(fdz):
```

REFERENCES

Aboudi, J. 2000. Micromechanical Prediction of the Effective Behavior of Fully Coupled Electro-Magneto-Thermo-Elastic Multiphase Composites. NASA/CR–2000-209787.

Aleksandrov, KS., Bondarenko, VS., Zaitzeva, MP., Sorokin, BP., Kokorin, YI., Zrazhevsky, VM. and Sobolev, BV. 1984. Nonlinear mechanical properties of sillenite type crystals. Soviet Journal of Solid State Physics (Physics of the Solid State, Moscow) 26:3603-3610, in Russian.

Alexe, M. and Goesele, U. 2003. Wafer Bonding, Springer, Berlin, Germany.

Al'shits, VI. and Lyubimov, VN. 1990. On existence of piezoelectric and piezomagnetic properties of anisotropic media. Soviet Krystallography (Moscow). 35(2):483-484, in Russian.

Anisimkin, IV. 2004. A type of acoustic modes of vibration of thin piezoelectric plates: quasi-longitudinal normal modes. Acoustical Physics Reports (Moscow). 50(4):442-447.

Bednarcyk, BA. 2002. A Fully Coupled Micro/Macro Theory for Thermo-Electro-Magneto-Elasto-Plastic Composite Laminates. NASA/CR–2002-211468, available electronically at http://gltrs.grc.nasa.gov/GLTRS.

Bleustein, JL. 1968. A new surface wave in piezoelectric materials. Applied Physics Letters. 13:412-413.

Blistanov, AA., Bondarenko, VS., Perelomova, NV., Strizhevskaya, FN., Chkalova, VV. and Shaskol'skaya, MP. 1982. Acoustical Crystals. Eds. Shaskol'skaya, MP. Nauka, Moscow, pp. 632, in Russian.

Bondarenko, VS., Zykov, AM., Polushkin, AN., Sergeev, AP., Sergeeva, GV. and Chkalova, VV. 1983. Application of layered system on fused-quartz for SAW delay lines. Materialy of Soviet Conference on Acoustoelectronics and Quantum Acoustics. Nauka, Saratov. 2:211-214, in Russian.

Bronstein, IN. and Semendyaev, KA. 2000. The reference-book on Mathematics for engineers and higher school students. Science, Moscow. pp.608, in Russian.

Cherednik, VI. and Dvoesherstov, MYU. 2003. Numerical calculation of surface and pseudo-surface acoustical wave features in multi-layered structures. Russian Journal of Technical Physics (Moscow). 73(10):106-112, in Russian.

Destrade, M. and Fu, YB. 2006. The speed of interfacial waves polarized in a symmetry plane. International Journal of Engineering Science 44:26-36.

Dieulesaint, E. and Royer, D. 1980. Elastic waves in solids: applications to signal processing, translated by Bastin, A. and M. Motz, Chichester [English]. J. Wiley, New York. pp511.

Dvoesherstov, MYU., Cherednik, VI., Chirimanov, AP. and Petrov, SG. 2003. Parameter optimization of surface acoustic waves by the way of multi-layered structures' usage. Russian Journal of Technical Physics (Moscow) 73(10):101-105, in Russian.

Farnell, GW. 1978. Types and properties of surface acoustical waves, in Acoustic Surface Waves. Topics in Applied Physics, Eds. Oliner, AA. Springer Verlag, Berlin-Heidelberg-New York. 24:26-96.

Farnell, GW. and Adler, EL. 1972. Elastic wave propagation in thin layers. in Physical Acoustics: Principles and Methods. Eds. Mason, WP. and Thurston, RN. Academic Press, New York. 9:35-127.

Goesele, U. and Tong, QY. 1998. Semiconductor wafer bonding. Annual Review of Material Science 28:215-241.

Gulyaev, YUV. 1969. Electroacoustical surface waves in solids. Soviet Physics Journal of Experimental and Theoretical Physics Letters (Moscow). 9:37-38.

Henaff, J., Feldmann, M. and Kirov, MA. 1982. Piezoelectric crystals for surface acoustic waves (Quartz, $LiNbO_3$, $LiTaO_3$, Tl_3VS_4, Tl_3TaSe_4, $AlPO_4$, GaAs). Ferroelectrics. 42:161-185.

Ingebrigtsen, KA. 1969. Surface waves in piezoelectrics. Journal of Applied Physics. 40(7):2681-2686.

Ivanov, LD. and Kessenikh, GG. 1987. Rayleigh surface wave in a transversally-isotropic substrate with rigid transversally-isotropic layer. Soviet Acoustical Journal (Moscow). 33(4):665-669, in Russian.

Jungnickel, F., Chillay, E., Makarov, S. and Froehlich, HJ. 1997. Coupling coefficient, temperature stability, and mass sensitivity of the Rayleigh-type mode on (001) [110] AlAs/GaAs. Smart Materials and Structures. 6:721-729.

Kolosovskii, EA., Tsarev, AV. and Yakovkin, IB. 1998. Improved procedure for measuring SAW velocity in anisotropic structures. Acoustical Physics Reports (Moscow). 44:793-800, in Russian.

Landolt-Boernstein International Tables. 1985. Elastic, piezoelectric, pyroelectric, piezooptic, electrooptic constants and non-linear dielectric susceptibilities of crystals, New Series, Group III, Vol. 18, Springer Verlag, Berlin–Heidelberg–New York–Tokyo. pp179.

Lardat, C., Maerfeld, C. and Tournois, P. 1971. Theory and performance of acoustical dispersive surface wave delay lines. Proceedings of the IEEE. 59(3):355-368.

Liu, H., Kuang, ZB. and Cai, ZM. 2003. Propagation of Bleustein-Gulyaev waves in a prestressed layered piezoelectric structure. Ultrasonics. 41:397-405.

Love, AEH. 1911. Some problems of Geodynamics, Cambridge University Press, London, England, UK.

Lyamov, VE. 1983. Polarization effects and interaction anisotropy of acoustic waves in crystals, MSU Publishing, Moscow. pp224, in Russian.

Nakamura, K. and Hanaoka, T. 1993. Propagation characteristics of surface acoustic waves in $ZnO/LiNbO_3$ structures. Japanese Journal of Applied Physics 32(5B-1): 2333-2336.

Nayfeh, AH. 1991. The general problem of elastic wave propagation in multilayered anisotropic media. Journal of Acoustical Society of America. 89:1521-1531.

Parygin, VN., Vershoubskiy, AV., Mozaev, VG. and Weinacht, M. 2000. Prolonged acousto-optic interaction with Lamb waves in crystalline plates. Ultrasonics 38: 594-597.

Pohanka, RC. and Smith, PL. 1988. Recent advances in piezoelectric ceramics. Electronic Ceramics. Eds. Levinson, LM. Marcel Dekker, New York, USA.

Rayleigh, Lord (J.W. Strutt), 1885. On waves propagated along the plane surfaces of an elastic solid. Proceedings of the London Mathematical Society. 17:4-11.

Schmidt, RV. and Voltmer, FW. 1969. Piezoelectric elastic surface waves in anisotropic layered media. IEEE Transactions on Microwave Theory and Techniques MTT. 17: 920-926.

Shiosaki, T., Yamamoto, T., Oda, T., Harada, K. and Kawabata, A. 1980. Low temperature growth of piezoelectric AlN film for surface and bulk wave transducers by RF reactive planar magnetron sputtering. in Proceedings of the IEEE Ultrasonics Symposium. 451-455.

Solie, LP. 1971. Piezoelectric acoustic surface waves for a film on a substrate. Applied Physics Letters. 18:111-112.

Solie, LP. and Auld, BA. 1973. Elastic waves in free anisotropic plates. Journal of Acoustical Society of America. 54(1):50-63.

Stoneley, R. 1955. The propagation of surface elastic waves in a cubic crystal. Proceedings of the Royal Society of London. A232:447-458.

Tsubouchi, K. and Mikoshiba, N. 1985. Zero-temperature-coefficient SAW devices on AlN epitaxial films. IEEE Transactions on Sonics and Ultrasonics SU. 32(5):634-644.

Tursunov, DA. 1967. Common surface waves in cubic crystals. Soviet Acoustical Journal (Moscow). 13:100-105, in Russian.

Volyansky, VF., Ivanov, LD., Kessenikh, GG. and Mogilevsky, ISH. 1987. Rayleigh surface wave in fused quartz substrate with AlN layer. Soviet Acoustical Journal (Moscow). 33(3):424-427, in Russian.

Yaralioglu, GG., Badi, MH., Ergun, AS., Cheng, CH., Khuri-Yakub, BT. and Degertekin, FL. 2001. Lamb wave devices using capacitive micromachined ultrasonic transducers. Applied Physics Letters. 78(1):111-113.

Zakharenko, AA. 2005[a]. Dispersive Rayleigh type waves in layered systems consisting of piezoelectric crystals bismuth silicate and bismuth germanate. Acta Acustica united with Acustica. 91(4):708-715.

Zakharenko, AA. 2005[b]. Analytical studying the group velocity of three-partial Love (type) waves in both isotropic and anisotropic media. Non-destructive Testing and Evaluation. 20(4):237-254.

Zakharenko, AA. 2006. On cubic crystal anisotropy for waves with Rayleigh-wave polarization. Non-destructive Testing and Evaluation. 21(2):1-17.

Zhang, B. and Lu, L. 2003. Rayleigh wave and detection of low-velocity layers in a stratified half-space. Russian Acoustical Journal (Moscow). 49(5):613-625, in Russian.

Zhang, VY., Lefebvre, JE. and Gryba, T. 2001. SAW characteristics in a layered ZnO/GaAs structure for design of integrated SAW filters. in Proceedings of the IEEE Ultrasonic Symposium, Atlanta, GA, USA, October. 1: 261-264.